

# Integrating Probabilities and Storylines to Explore Uncertain Direct and Cascading Climate Risks in Multi-sectoral Systems: A Case of The Lielupe Basin

Franciscus Eduard Buskop<sup>1,2</sup>, Frederiek Sperna Weiland<sup>2</sup>, Stefan Hochrainer-Stigler<sup>3</sup>, Robert Šakić Trogrlić<sup>3</sup>, and Bart van den Hurk<sup>1,2</sup>

<sup>1</sup>Vrije Universiteit Amsterdam

<sup>2</sup>Deltares

<sup>3</sup>IIASA-International Institute for Applied System Analysis

January 11, 2025

## Abstract

Anticipating and managing future climate risks in interconnected multi-sectoral systems is complicated by uncertainties in risk drivers in both human and natural systems. Comprehensive yet comprehensible targeted climate risk information exploring these uncertainties is relevant for e.g. strategic allocation of limited resources to the most vulnerable areas and sectors. To address these complexities, this study introduces an interdisciplinary methodology combining meteorological, hydrological, and socio-economic perspectives, tested in the flood-prone, transboundary Lielupe basin shared by Latvia and Lithuania. A 'plausibilistic' risk assessment approach is applied in which plausible climate scenario storylines are sampled on their relevance for local impacts, allowing the assessment of conditional changes in high-impact probabilistic discharges. In addition, plausible yet differently structured future urban areas and economies are sampled to project direct impact potential and its cascading socio-economic effects. By integrating both climate and socio-economic scenarios, a risk mapping can be made to highlight regions where (compounding) risk drivers may occur. Application to the Lielupe basin reveals those areas and sectors most vulnerable to climate impacts across diverse climate and socio-economic scenarios. Our comprehensive approach equips regional risk managers with targeted risk information essential for prioritising adaptation planning.

## Hosted file

Manuscript\_uncertain\_regional\_direct\_sectoral\_climate\_risks\_2024\_12\_20.docx available at <https://authorea.com/users/876284/articles/1256167-integrating-probabilities-and-storylines-to-explore-uncertain-direct-and-cascading-climate-risks-in-multi-sectoral-systems-a-case-of-the-lielupe-basin>

# Integrating Probabilities and Storylines to Explore Uncertain Direct and Cascading Climate Risks in Multi-sectoral Systems: A Case of The Lielupe Basin

F.E. Buskop<sup>1,2,3</sup>, F. Sperna Weiland<sup>2</sup>, S. Hochrainer-Stigler<sup>3</sup>, R. Šakić Trogrlić<sup>3</sup> and B.J.J.M. van den Hurk<sup>1,2</sup>

<sup>1</sup>Institute for Environmental Studies, Vrije Universiteit Amsterdam, Amsterdam, The Netherlands

<sup>2</sup>Deltares, Delft, The Netherlands

<sup>3</sup>IIASA - International Institute for Applied Systems Analysis, Laxenburg, Austria

Corresponding author: Franciscus Eduard Buskop ([t.buskop@vu.nl](mailto:t.buskop@vu.nl))

## Key Points:

- A 'plausibilistic' approach to assess uncertain regional climate risks by combining event probabilities and plausible climate storylines
- Targeted insights addressing direct and cascading risks in multi-sectoral systems facing climate and socio-economic uncertainty
- Application to the Lielupe basin highlights key risk areas and sectors, aiding risk managers in their adaptation planning

## Abstract

Anticipating and managing future climate risks in interconnected multi-sectoral systems is complicated by uncertainties in risk drivers in both human and natural systems. Comprehensive yet comprehensible targeted climate risk information exploring these uncertainties is relevant for e.g. strategic allocation of limited resources to the most vulnerable areas and sectors. To address these complexities, this study introduces an interdisciplinary methodology combining meteorological, hydrological, and socio-economic perspectives, tested in the flood-prone, transboundary Lielupe basin shared by Latvia and Lithuania. A 'plausibilistic' risk assessment approach is applied in which plausible climate scenario storylines are sampled on their relevance for local impacts, allowing the assessment of conditional changes in high-impact probabilistic discharges. In addition, plausible yet differently structured future urban areas and economies are sampled to project direct impact potential and its cascading socio-economic effects. By integrating both climate and socio-economic scenarios, a risk mapping can be made to highlight regions where (compounding) risk drivers may occur. Application to the Lielupe basin reveals those areas and sectors most vulnerable to climate impacts across diverse climate and socio-economic scenarios. Our comprehensive approach equips regional risk managers with targeted risk information essential for prioritising adaptation planning.

## Plain Language Summary

Understanding future climate risks, like flooding, is crucial but challenging due to uncertainties in how both the climate and human societies will evolve. It is, therefore, important to consider

37 a range of plausible risk futures. Our study introduces a new method to sample a limited yet  
38 comprehensive range of possible risk futures, providing targeted information to help decision-  
39 makers prepare for an uncertain future. By combining climate and socio-economic  
40 perspectives, we identify areas where direct flood risks are likely to change and assess how  
41 these changes could ripple through the economy. We tested this approach in the flood-prone  
42 Lielupe river basin, shared by Latvia and Lithuania. We analysed potential shifts in extreme  
43 flood discharges and their impacts using various scenarios of relevant future climate conditions,  
44 urban development, and economic changes. The findings reveal that flood risks can vary  
45 significantly across regions and sectors, depending on the combination of climate and socio-  
46 economic conditions and resulting risk drivers. Our approach allows policymakers to find those  
47 areas and sectors most vulnerable across diverse scenarios, offering valuable insights for  
48 prioritising targeted adaptation strategies.

## 49 **1 Introduction**

50 As climate impacts intensify throughout the twenty-first century (Mora et al., 2013), regions  
51 across the globe increasingly need targeted climate risk information to inform adaptation plans  
52 that protect vulnerable areas and sectors. Unfortunately, future climate risk information is  
53 obscured by large uncertainties in future climate conditions due to unknowns in emission  
54 pathways (O'Neill et al., 2017; van Vuuren et al., 2011), earth system responses to those  
55 emissions (Hawkins & Sutton, 2011; F. Lehner et al., 2020) and societal developments (O'Neill  
56 et al., 2014; Wilby & Dessai, 2010). To assess this uncertainty and convert it into a manageable  
57 risk information package serving the design of effective adaptation strategies, a subset of  
58 plausible climate impact scenarios can be explored to inform robust decision-making (Lempert,  
59 2013; Lempert et al., 2003) or adaptive planning approaches (Haasnoot et al., 2019).

60 One method to explore impact uncertainty is through physical climate storylines (Shepherd,  
61 2019; Shepherd et al., 2018), where lessons can be learned from 'what if' scenarios and their  
62 conditional explanations (Sillmann et al., 2021). By exploring multiple storylines that  
63 incorporate climate change or socio-economic developments, one can find vulnerabilities and  
64 drivers of risks that require specific attention (Goulart et al., 2024; van den Hurk et al., 2023).  
65 One application of climate storylines is to explore plausible changes in conditional probabilities  
66 of extreme meteorological events for the selected climate storylines (Liné et al., 2024; van den  
67 Hurk, 2022; van der Wiel et al., 2024). Such probabilities (or likelihoods) are an important factor  
68 for investment decisions in either risk prevention, consequence reduction, or risk transfers  
69 (Linnerooth-Bayer & Hochrainer-Stigler, 2015; Mechler et al., 2014). However, quantitative  
70 estimates of changes in impact probabilities, which require an interdisciplinary approach, have  
71 remained elusive in current literature.

72 Climate scenario storylines such as those of Liné et al. (2024) take a meteorological perspective  
73 to storyline construction, aiming to cover the variability of a broad set of 'target weather  
74 variables' conditioned on a few large-scale Earth system characteristics such as the North  
75 Atlantic Oscillation (NAO) or Atlantic meridional overturning circulation (AMOC). Conversely,  
76 Van der Wiel et al. (2024) construct storylines conditioned on the direct local precipitation  
77 response while aiming to describe a large set of associated target weather variables to serve a  
78 broad group of stakeholders. Although this approach has merit in providing climate scenarios  
79 for many, such generic scenarios may lack specificity for individual decision-making contexts  
80 since information needs are not uniform throughout society (Kirchhoff et al., 2013).  
81 Information salience is one of the key requirements for decision-making (Lemos et al., 2012),  
82 requiring appropriate methods to provide such information. Climate scenario storylines  
83 targeting variables directly related to the impacts on specific stakeholders have the potential to  
84 provide effective insights into the local implications of climate change (Sillmann et al., 2021).

85 Additionally, climate impacts occur in an increasingly connected world where direct effects in  
86 one region or industry can cascade through to connected industries or regions (Middelanis et  
87 al., 2021; Sieg et al., 2019). As a result, systemic risk assessments are essential to inform  
88 adaptation measures that comprehensively mitigate the various risk mechanisms in multi-  
89 sector systems (Challinor et al., 2018; Hochrainer-Stigler et al., 2023; Levermann, 2014). While

90 indirect or cascading societal effects induced by climate hazards have been analysed for future  
91 climate conditions in several studies (Lawrence et al., 2020; Willner et al., 2018), to the best of  
92 the author's knowledge, none have sought to explore the cascading effects of climate shocks in  
93 future socio-economic scenarios, despite evidence in Leimbach et al. (2023) that economies  
94 and their compositions can change over time. Changes in sector interactions may contribute  
95 considerably to the occurrence of indirect effects of climate shocks.

96 To address identified limitations in the current storyline literature, we propose and test a novel  
97 multi-modal methodology designed to provide targeted, conditional probabilistic climate  
98 impact information for plausible climate and socio-economic storylines. We term this  
99 integrated approach 'plausibilistic,' as it merges probabilistic hazard information with plausible  
100 storylines. By separating impacts into direct and cascading effects, a rich and comprehensive  
101 overview can be obtained of future risks in uncertain multi-sectoral human-natural systems.  
102 Our methodology focuses on identifying locally relevant impact drivers, which guide the  
103 selection of relevant storylines from the wide range of possible climates and socio-economic  
104 projections. Within each storyline, we map regional impact drivers and illustrate where these  
105 drivers potentially compound. Furthermore, we analyse which economic sectors experience the  
106 most severe stress after a climate shock and how this changes in various conditions.

107 To demonstrate the utility of the presented methodology, we test it in an illustrative case. We  
108 focus on flood risk as it is one of the key risks throughout Europe in a changing climate (Bednar-  
109 Friedl et al., 2022; European Environment Agency, 2024). An exemplary case is the  
110 transboundary Lithuanian-Latvian Lielupe, where flood risk is already a prominent issue and is a  
111 core focus of the Latvian National Adaptation Plan (Ministry of Environmental Protection and  
112 Regional Development, 2019). We, therefore, apply and test the framework in a riverine flood  
113 risk case in the Lielupe basin.

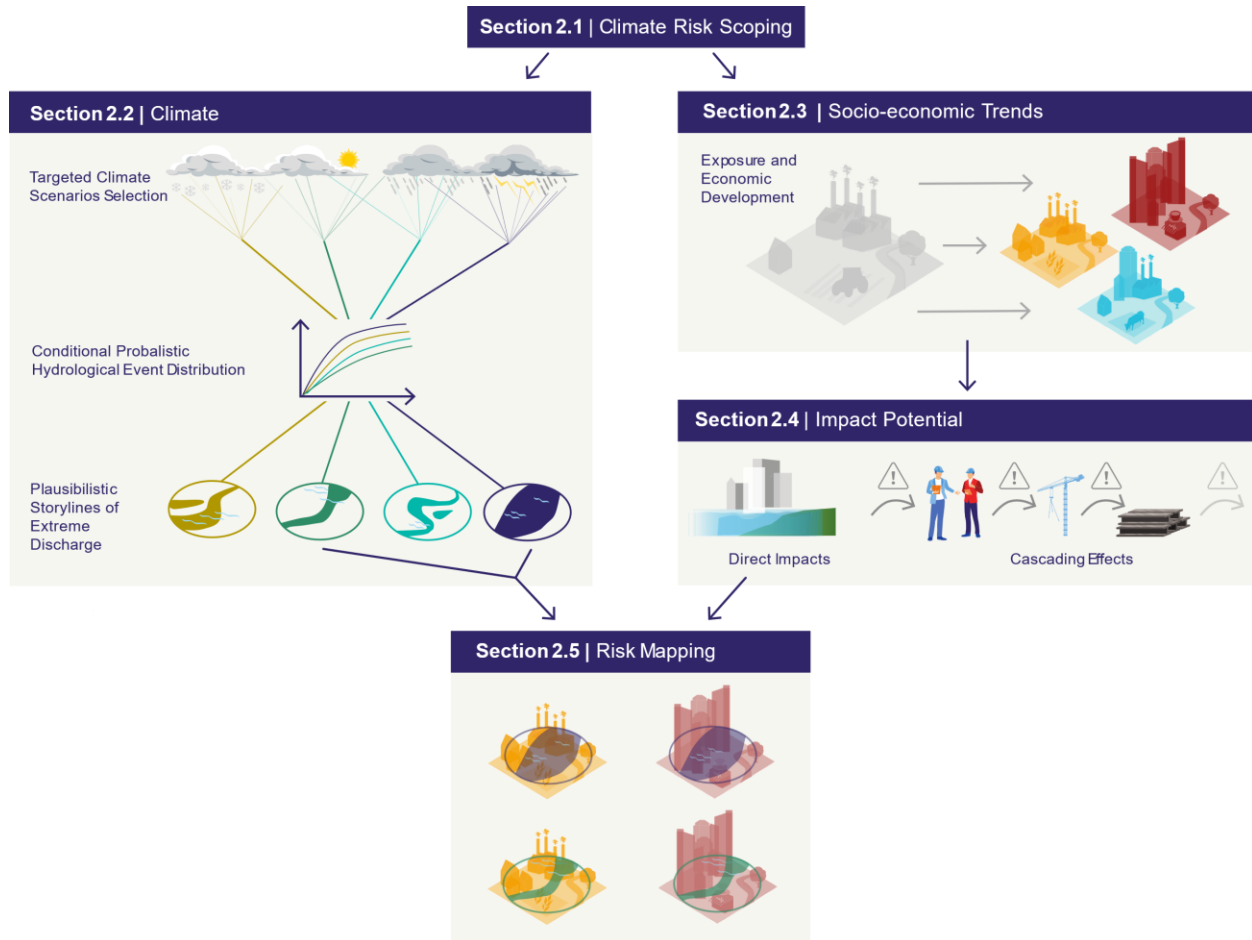
## 114 **2 Method**

115 This study aims to provide a comprehensive assessment of future flood risk impacts in multi-  
116 sectoral systems by sampling from a range of projections differentiating emission scenarios,  
117 Earth system responses, internal variability, and societal development. We follow the multi-  
118 model experimental design depicted in Figure 1. The analysis starts with climate risk scoping,  
119 where the key issue of interest is defined, and the boundaries of the analysis are set (Section  
120 2.1). Secondly, we examine how climate uncertainties influence extreme discharges across the  
121 basin (Section 2.2). This analysis starts by crafting plausible climate scenario storylines from an  
122 ensemble of Global Climate Model projections based on locally relevant Climatic Impact Drivers  
123 (CIDs) revealed by a sensitivity analysis. For each climate storyline, conditional probabilistic  
124 extreme discharges are determined using hydrological modelling and stochastic weather  
125 generation. The resulting plausibilistic storylines of extreme discharge are spatially mapped to  
126 gain insight into regional and inter-storyline differences in local flood risk.

127 In parallel, the propagation of direct flood impact to indirect economic repercussions is  
128 analysed in multiple projections of plausible socio-economic developments influencing exposed  
129 building asset values and relevant sectors in the region. These socio-economic projections

130 provide perturbations to the exposure characteristics in regional floodplains and modify  
 131 economic structures and, consequently, sectoral interactions (Section 2.3). Comparing direct  
 132 impacts and resulting cascading effects across scenarios illustrates how sectoral and regional  
 133 stresses can potentially evolve, allowing the identification of those areas and sectors whose  
 134 direct and indirect flood risks are most affected by socio-economic changes (Section 2.4).

135 Lastly, the plausible discharge storylines and socio-economic scenarios are overlaid to  
 136 identify those locations where risk drivers compound, providing a risk mapping under future  
 137 conditions (Section 2.5).



138  
 139 **Figure 1:** Methodology used in the study to gain insight into future climate impacts for the specified  
 140 climate challenge.

141 **2.1 Climate Risk Scoping**

142 The first step of our methodology is to define and scope the regional climate risk of interest.  
 143 This step involves identifying the region, hazard type, impacts, sectors, and time horizon, which  
 144 collectively influence the conclusions drawn in risk analysis. Points of departure for our analysis  
 145 are the Latvian National Adaptation Plan (NAP) (Ministry of Environmental Protection and  
 146 Regional Development, 2019) and river basin management plans (Latvijas Vides, ģeoloģijas un

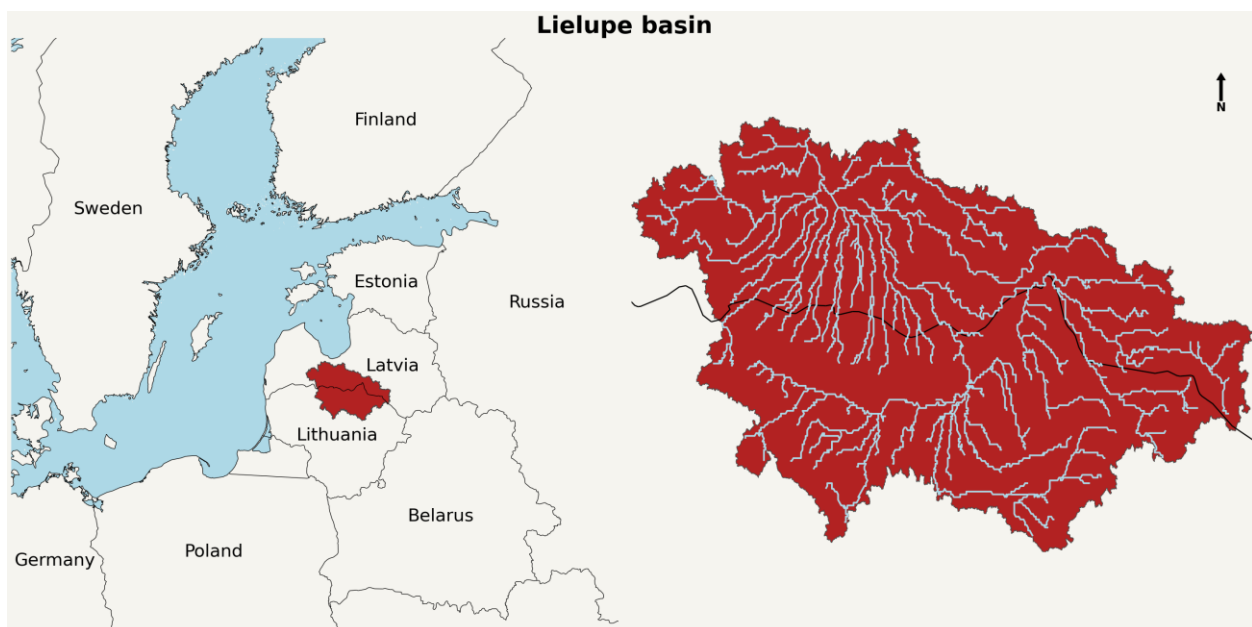
147 meteoroloģijas centrs, 2023). These documents are intended to support regional planning in  
148 the upcoming decade, and as such, information about potential risk developments during the  
149 mid-century is of particular interest.

150 The NAP voices concerns about flooding along rivers in the country. One such flood area is the  
151 transboundary Lielupe Basin (Figure 2). The Latvian-Lithuanian basin covers 17.600km<sup>2</sup> and  
152 houses around 400.000 people. Local authorities have identified parts of the basin as a current-  
153 day flood zone of national importance, and therefore, information on near-future flood risk is  
154 highly valuable. Especially the 1/100-year return period flooding is of interest, as events of this  
155 intensity cause significant impacts in the region. Both the NAP and river basin management  
156 plan are particularly concerned regarding losses to constructed assets, in our case buildings,  
157 along rivers. Consequently, this study will aim to provide risk developments regarding these  
158 assets.

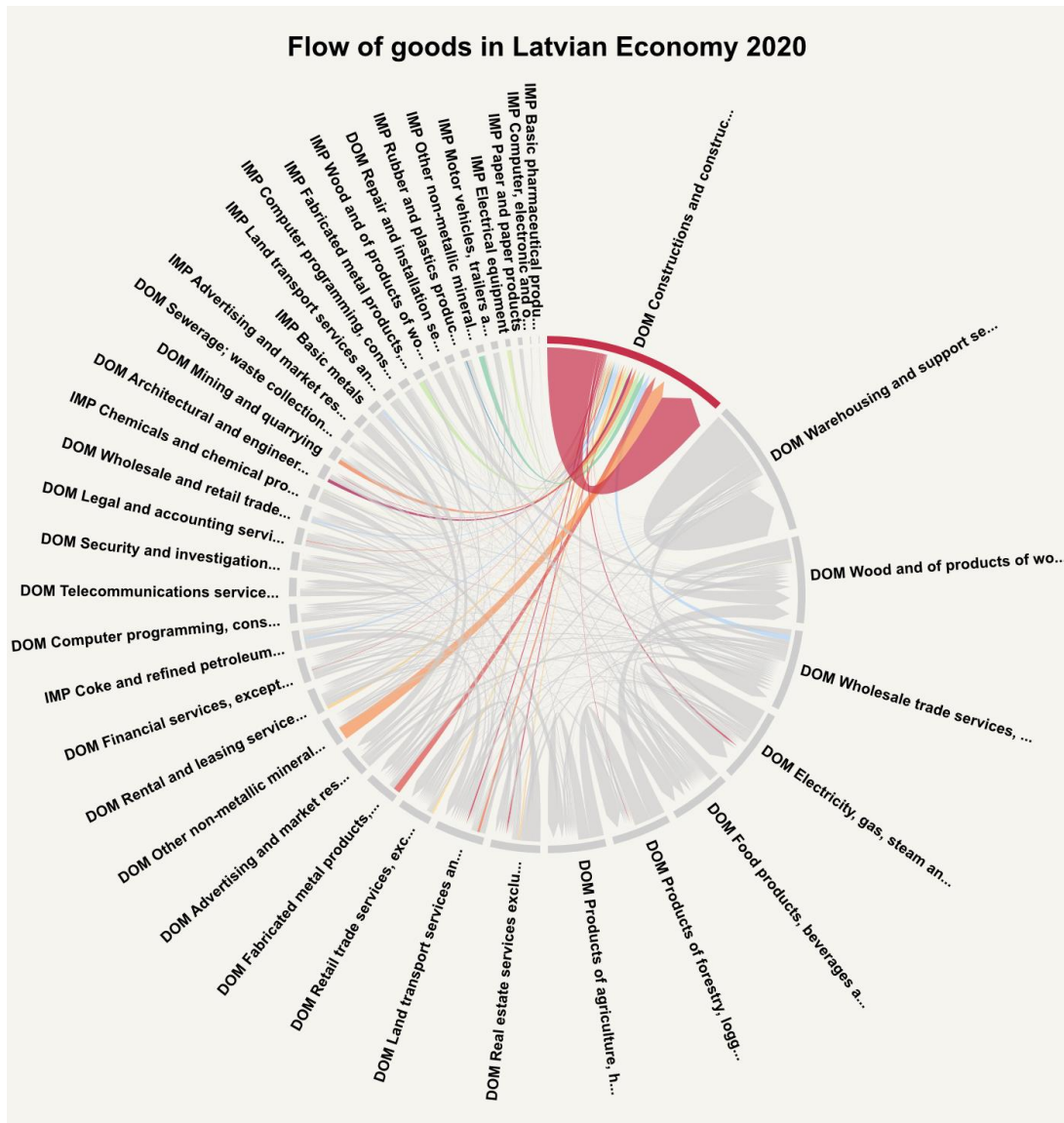
159 These direct flood impacts on buildings have the potential to affect economic sectors outside of  
160 the flood area. To illustrate the potential of cascading effects, Figure 3 shows the flow of goods  
161 between sectors for the region, revealing intersectoral dependencies. The construction sector  
162 and its direct to suppliers and consumers in the economy are particularly highlighted, because  
163 it is Latvia's largest producer and consumer of goods and depends on many domestic and  
164 foreign sectors, and has a large importance in the national economy. It is arguably an important  
165 sector in rebuilding flood-impacted assets, so it is relevant to investigate the direct and indirect  
166 effects around this sector.

167 In summary, this study will analyse plausible climate impact storylines for the 1/100-year  
168 return period flood event, its direct impact on building assets and the cascading effects in the  
169 Latvian economy for the mid-century.

170



172 **Figure 2:** Region of interest. The left image shows the location in Europe, and the right image is a more  
 173 detailed image of the river network in the basin. The red-filled shape is the Lielupe basin, and light blue  
 174 indicates the sea surface and the rivers.



175  
 176 **Figure 3:** Sectoral interdependencies of the 40 largest sectors in Latvia based on the sum of intermediate  
 177 sectoral consumption and production of goods in euro. Sectors are sorted on flow sums from large to  
 178 small in a clockwise position. Arrows indicate the direction of goods. The studied construction sector and  
 179 its direct supplier and customer streams are highlighted in colour. Underlying data is obtained from the  
 180 Latvian statistics portal (Central Statistical Bureau of Latvia, 2023). "DOM" indicates domestic sectors, while "IMP"  
 181 represents imported products, highlighting the distinction between locally produced and imported sectoral impacts.

## 182 2.2 Plausibilistic storylines of extreme discharge

183 Analysing how extreme discharges change in the basin is a key component of mapping future  
 184 risks. However, these extremes are dependent on uncertain future climate conditions. For the

185 Lielupe case, we specified a sub-selection of plausible mid-century climate scenario storylines,  
186 and calculated changes in the conditional probabilistic 1/100 return period discharge for each  
187 storyline relative to the current baseline.

188 To obtain this information, this study replicates and extends the method introduced by Buskop  
189 et al. (2024). This method creates a set of four climate scenario storylines by clustering GCM  
190 projections based on modelled changes in locally relevant CIDs, instead of clustering by  
191 emission scenario. Projections of local precipitation patterns are primarily governed by internal  
192 variability and model uncertainty (Hawkins & Sutton, 2011; F. Lehner et al., 2020), and  
193 aggregation by emission scenario leaves hardly any meaningful scenario variability for exploring  
194 regional climate risks. As such, a relevant range of potential future conditions combines the  
195 effects of internal variability, model uncertainty, and emission pathways to be used in regional  
196 disaster risk management and adaptation planning (Deser, 2020).

### 197 **2.2.1 Relevant Climatic Impact Drivers in the Basin**

198 To develop climate scenario storylines that allow us to explore a range of plausible extreme  
199 discharge changes in the basin, we use the method detailed by Buskop et al. (2024). The  
200 method starts by identifying CIDs that significantly influence flood risk in the region. Using  
201 these CIDs, flood-relevant climate scenario storylines can be constructed (section 2.2.2).  
202 Relevant CID identification requires the development of atmospheric forcing time series under  
203 various climate conditions, a calibrated hydrological model to capture resulting discharge  
204 extremes, and a feature scoring step that identifies those CIDs that influence extreme  
205 discharges most.

206 Meaningful hydrological modelling of discharge extremes requires high resolution, forcing time  
207 series of daily temperature and precipitation. At the same time, comparing the influence of  
208 CIDs on discharge extremes requires a consistent sequence of events across alternative forcing  
209 runs. These two requirements are currently unavailable in the available GCM time series. To  
210 this end, a stochastic weather generator based on Steinschneider and Brown (2013) is used.  
211 ERA5 data (Hersbach et al., 2023) informs the weather generator to create a 100-year-  
212 long synthetic baseline time series of temperature and precipitation in the region. Alternative  
213 climatological forcing conditions are created by modifying the baseline time series seasonal  
214 mean temperature ( $\Delta T$ ), mean rainfall ( $\Delta P$ ) and the coefficient of variation ( $\Delta CV$ ) of that rainfall.  
215 These changes are informed by CMIP6 GCM projections available at the Copernicus Climate  
216 Data Store (Copernicus Climate Change Service, 2021), also see Appendix A. Change signals for  
217 the mid-century as defined in the IPCC atlas, 2041-2060 (Gutiérrez et al., 2021), are retrieved  
218 across four seasons: winter (December-January-February), spring (March-April-May), summer  
219 (June-July-August) and autumn (September-October-November). The hydrological model  
220 Wflow\_sbm (van Verseveld et al., 2024) is configured using model builder HydroMT (Eilander et  
221 al., 2023). Using the alternative forcing time series and the hydrological model, discharge  
222 extremes are calculated for each climate condition. The Extra Trees feature scoring algorithm  
223 (Geurts et al., 2006) is applied to link simulated changes in extreme discharge to associated  
224 changes in CIDs, identifying the most influential CIDs in determining these discharge variations.

225 To create climate scenarios that are relevant across the basin, it is necessary to know which  
226 combination of CIDs changes flood risk at a variety of locations. For this, we extended the  
227 approach of Buskop et al. (2024) from a single-point location analysis of discharge change to a  
228 spatial, basin-wide application. Discharge changes are collected at observation stations, where  
229 the hydrological model fairly replicates historical discharge ( $KGE \Rightarrow 0.5$ ). For each of these  
230 stations, the two most influential CIDs that alter extreme discharge are determined as  
231 described by Buskop et al. (2024). This results in a list of CIDs that influence flood risk across the  
232 basin. After removing duplicates from the list, we cluster the GCMs into four clusters based on  
233 the projected changes for each CID in the list.

### 234 **2.2.2 Climate scenario storylines and their conditional probabilistic extreme discharges**

235 Each GCM cluster is transformed into climate scenario storylines by calculating the cluster's  
236 multi-model average climate change signal for the sampled climate variables ( $\Delta T$ ,  $\Delta P$ ,  $\Delta CV$ ) in  
237 each season. The four distinct climate storylines are then used to discover future discharge  
238 changes across the basin. For each constructed climate storyline, new 100-year-long stochastic  
239 weather time series are created. This is done by modifying the baseline time series by each  
240 climate storyline's precipitation and temperature change signals. Since weather generators are  
241 subject to sampling uncertainty (Alodah & Seidou, 2020), five alternative realisations have been  
242 created and used as forcing to the hydrological model. For each realisation of a climate  
243 storyline, the fractional change in the 1/100-year return period discharge relative to the control  
244 baseline is calculated. These change values are averaged across realisations to obtain the  
245 discharge change in the storylines to be used in further analysis.

246 For each climate storyline, basin-wide probabilistic discharge changes are calculated and  
247 mapped using the HydroSheds classification of sub-catchments (B. Lehner & Grill, 2013). The  
248 resulting map provides a spatial representation of hazard intensity changes per hydrological  
249 run, revealing potential differences across catchments. We call this set of discharge event  
250 changes 'plausibilistic storylines of extreme discharge' that span a range of GCM projections  
251 and resulting impacts.

### 252 **2.3 Socio-economic trends**

253 Socio-economic changes in a region significantly contribute to changes in overall climate risk  
254 (Dottori et al., 2018; Steinhausen et al., 2022) as they alter regional exposure and vulnerability  
255 and should be included in regional climate risk assessments. For direct risks, we explore how  
256 exposure and, therefore, the impact potential in each sub-catchment develops into the future.  
257 Specifically, this study focuses on building exposure values (Section 2.31). For cascading effects  
258 throughout the economic network, we construct perturbed regional economic networks by  
259 changing future sectoral production and consumption volumes and their interdependencies  
260 (Section 2.3.2). Both developments in the exposure and economic network are guided by the  
261 Shared Socio-economic Pathways (SSP) framework (O'Neill et al., 2014, 2017). Multiple SSPs are  
262 used to explore the uncertainty range in regional socio-economic trends. By using the SSP  
263 framework we can combine studies that are based on the SSPs in a way that projected variables

264 are consistent with each other. To reflect our localised application, we further refer to these  
265 SSP-inspired scenarios as 'regional economic futures'.

### 266 **2.3.1 Asset development in the region**

267 To assess changes in direct impacts, we explore the change in building value exposure over time  
268 as it is a key driver of risk. Direct impacts are modulated by altering each sub-catchment's total  
269 area occupied by building footprints and the cost of rebuilding a structure. We calculate these  
270 changes in exposed asset values in the regions by using global datasets of downscaled spatial  
271 projections of GDP growth (Wang & Sun, 2022), urban density (Gao & Pesaresi, 2021), and  
272 urban expansion (Chen et al., 2020) at 1 km spatial resolution. These datasets disaggregate  
273 national-level Gross Domestic Product (GDP), population, and urbanisation based on current  
274 population and GDP distributions, where built-up areas aggregate a larger fraction of the  
275 projected changes than countryside areas. By multiplying the GDP growth with urban density  
276 change and urban expansion in a sub-catchment, we obtain the asset value change factor that  
277 is used to project the asset values in the floodplains between the 2020 baseline and 2050 (see  
278 Section 2.4.1).

### 279 **2.3.2 Scaling sectors and their interdependencies**

280 Cascading effects in the economic system are influenced by how individual sectors develop and  
281 how sectors interact. Changes in cascading effects are assumed to be related to socio-economic  
282 trends in GDP and the contribution of individual sectors to that GDP. These factors allow us to  
283 analyse changing national economic structure, sectoral dependencies and, consequently,  
284 cascading impacts of flood events. National GDP projections under various global SSP scenarios  
285 exist for some time (Dellink et al., 2017) and have been used before to downscale GDP  
286 projections (Wang & Sun, 2022). However, a decomposition into sectoral contributions has only  
287 been introduced recently by Leimbach et al. (2023). Figure 4 shows various pathways of GDP  
288 development and sectoral contributions.

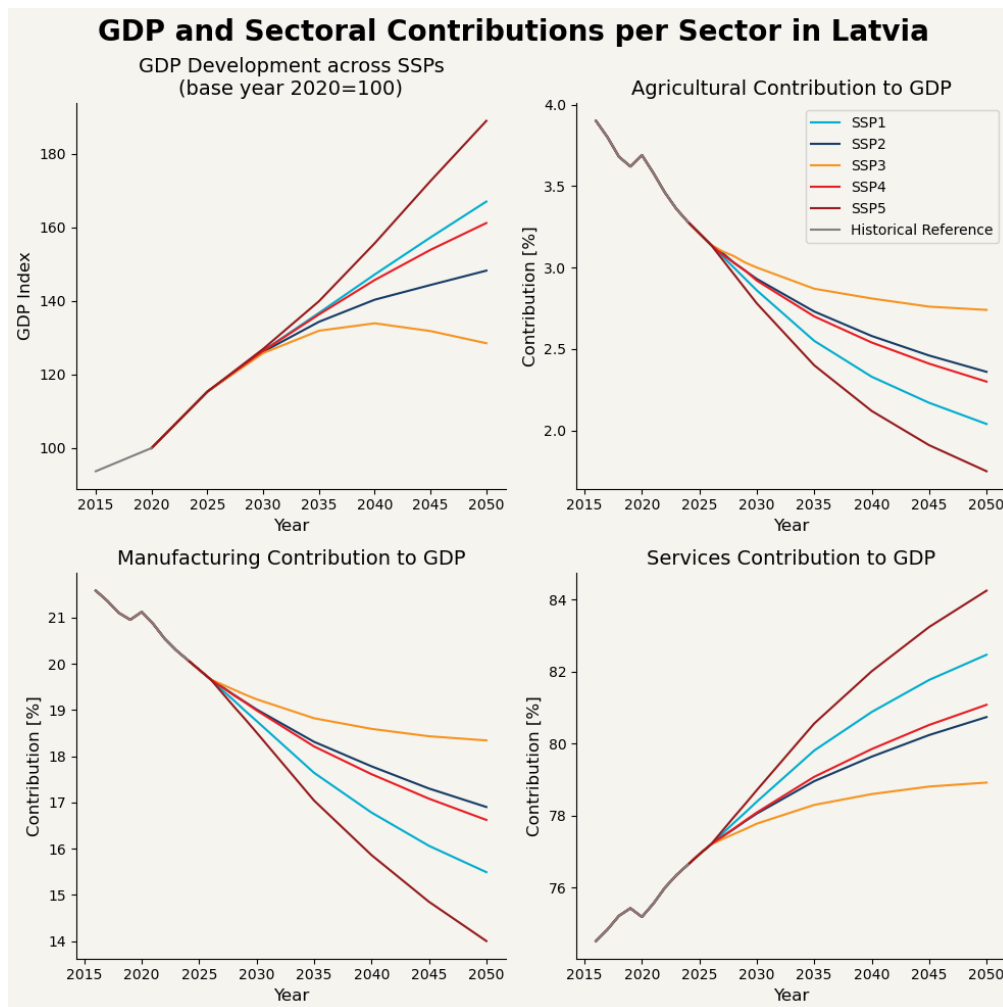
289 To obtain new sectoral interactions and production quantities in 2050, we project national  
290 input-output tables for each economic scenario. Input-output tables, introduced by Leontief  
291 (1936), are a common way for government statistical agencies to collect and describe the  
292 relationships between sectors within a country and sectors abroad by documenting the  
293 monetary value of the flow of goods between sectors. These tables thus describe how much  
294 each sector supplies to and consumes from other sectors. Using these tables, ripple effects  
295 from one sector to another can be tracked. In climate science, input-output tables have been  
296 used in a variety of studies covering the indirect effects of supply losses after flooding (Sieg et  
297 al., 2019), accounting of environmental footprints, including global trade (Tukker et al., 2016),  
298 and post-disaster dynamics in the economy (Koks & Thissen, 2016; Middelani et al., 2021).

299 We project national input-output tables using socio-economic trends and sectoral shifts  
300 depicted in the SSPs. Starting with the 2020 Latvian input-output table containing 64 NACE  
301 sectors, we aggregate these into three NACE3 sectors (Agriculture, Manufacturing, and  
302 Services) to align with Leimbach et al.'s (2023) projections. The NACE nomenclature is a

303 standardised system in the European Union to classify and aggregate economic activities  
 304 (Eurostat, 2008). The projection calculation starts by scaling the 2020 national value added to  
 305 2050 GDP levels and allocating it to sectors proportional to projected contributions shown in  
 306 Figure 4. We then disaggregate back to NACE64 sectors using 2020 ratios, calculate required  
 307 input goods, and scale final demands with GDP growth.

308 To address imbalances between growing and shrinking sectors, we implement a balancing  
 309 mechanism within the input-output framework. When domestic sectors cannot meet increased  
 310 demand, we introduce additional imports distributed according to current-day usage shares.  
 311 Conversely, when local production exceeds demand, we reduce imports according to usage  
 312 shares with a minimum of zero imports. We convert the surplus production into exports. This  
 313 balancing process ensures that sectoral inputs and outputs align. The end results are input-  
 314 output projections per regional economic future suitable for analysing the cascading effects of  
 315 flood events. See Appendix B for detailed explanations and formulas describing the  
 316 calculations.

317



318

319 **Figure 4:** GDP development and sectoral contributions. Top left panel: GDP development index across various  
320 global SSPs (100 = GDP in base year 2020). Other panels show changes in the composition of the Latvian economy.  
321 Each plot shows the change in the contribution of a specific sector to Latvian GDP. Data obtained from the IIASA  
322 SSP Extensions Explorer (Andrijevic et al., n.d.) and IIASA SSP Scenario Explorer (<https://data.ece.iiasa.ac.at/ssp>)

## 323 2.4 Impact potential

### 324 2.4.1 Exposed assets in the floodplain

325 Direct flood impact potential is estimated by evaluating asset values within the floodplains. To  
326 identify the floodplain for each sub-catchment, we use 50-meter resolution historical flood  
327 extent maps created by local authorities. The flood extent for the highest available return  
328 period under current climate conditions is used. Since the basin covers two countries, we had  
329 to harmonise the 200-year return period flood map for Latvia and the 1000-year return period  
330 map for Lithuania to a regional product. This leads to better agreement with local maps than  
331 utilising harmonised European or global datasets for multiple low-probability return periods  
332 (e.g. Dottori et al. (2022) or Aqueduct (Ward et al., 2020)), which may let water reach locations  
333 that are inaccessible in reality leading to misrepresented areas at risk. We attribute this low  
334 agreement to the fact that the Lielupe basin contains levees and weirs to control floods. These  
335 structures are likely to be too small to be picked up by coarse large-scale flood modelling  
336 efforts.

337 Current-day exposure values in the floodplains are estimated using empirical estimates of  
338 reconstruction costs per square meter identified by Huizinga et al. (2016). The reconstruction  
339 costs need to be defined per building and its use class, since each use class has a different  
340 associated cost. Using OpenStreetMap (OSM) (Haklay & Weber, 2008), flooded building  
341 footprints are obtained and assigned a use class. First, we classify all footprints as residential,  
342 refine them using the 50x50m LUISA land use dataset (Pigaiani & Batista e Silva, 2021) and  
343 refine further with OSM land use and amenity information (see Appendix C Table C.1 and C.2  
344 for the classifications). Lastly, the total footprint areas are calculated and multiplied by the  
345 reconstruction costs per square meter to obtain exposed asset values in the floodplain. Content  
346 losses are not considered since our focus is on reconstruction.

347 To incorporate socio-economic trends in the assessment, current exposure values per sub-  
348 catchment are adjusted to future values. We incorporated urban growth and property value  
349 growth by multiplying current exposure in the sub-catchment with their projected change  
350 factor, found in Section 2.3.1.

### 351 2.4.2 Indirect effects

352 A relevant indirect impact of flood risk is the pressure on sectors to substitute what was lost. If  
353 these sectors are overwhelmed by the extent of the event and the resulting increased demand,  
354 this can lead to enhanced and prolonged impacts (Hallegatte et al., 2024). To highlight potential  
355 reconstruction issues in the recovery phase, this study analyses cascading sectoral pressures  
356 directly after an applied shock for the 2020 baseline and the various regional economic futures.  
357 We use 'stress' to indicate demand pressures due to the event relative to the pre-event

358 demand for a sector. Sectors are ranked by their demand stresses in 2020 conditions, and we  
359 explore how these stresses develop across scenarios.

360 Input-output tables are used to explore sectoral demand change effects throughout the  
361 economy (Miller & Blair, 2009). The monetary interconnections between sectors in these tables  
362 are manipulated to show economy wide effects of a demand shock in the construction sector  
363 after a flood. We implemented this manipulation by calculating the Leontief inverse matrix  
364 (Leontief, 1936), which formulates the economy-wide input requirements for each sector to  
365 produce one output unit of the sector, including cascading demand effects from suppliers. For a  
366 formulaic representation of the demand changes, see Appendix D.

367 We find stresses across the Latvian economy by applying an arbitrary demand on the  
368 construction sector resulting from direct losses. Using the Leontief inverse, we find how much  
369 pressure occurs in the construction sector and its supply chain. Instead of absolute demand  
370 increases, relative demand increases are explored as they signal stresses on the sectors. Those  
371 sectors that need to upscale production most are particularly vulnerable to indirect flood  
372 impacts.

373 To compare baseline conditions with future scenarios, we perform the analysis for the base  
374 year 2020 and all regional economic futures in 2050 using associated input-output tables (see  
375 Section 2.3.2) and the growth of asset values in the floodplain (see Section 2.4.1). The set of  
376 input-output tables provides estimates of sectoral interactions and the relative size of sectors in  
377 the regional economy. The asset value growth in the floodplain is used to compare how a single  
378 unit of loss in 2020 is expected to grow in the future.

## 379 **2.5 Compounding Impact Drivers**

380 The identified plausible extreme discharge storylines and socio-economic developments can  
381 be integrated to find those regions most vulnerable to future climate impacts. Using the  
382 exposure to direct impacts and discharge change for each sub-catchment, a climate risk  
383 mapping can be performed. Sub-catchments, where both impact potential and extreme  
384 discharge increases, are highest are assigned the highest risk level. A comprehensive overview  
385 of potential future risks can be made by making combinations of the plausible discharge  
386 storylines with socio-economic developments.

387 Whereas global and continental scale risk assessments often couple RCPs and SSPs, we choose  
388 to let climate and socio-economic scenarios vary independently of each other for this regional  
389 study. For large-scale risk assessments, coupling is intuitive since a specific global emissions  
390 level can only occur when there is a specific global socio-economic development (van Vuuren et  
391 al., 2014). However, local socio-economic developments can diverge substantially from global  
392 trends governing climate change processes, driven by local policies and economic conditions. In  
393 addition, our scenario framework does not scale with global greenhouse gas emissions (also  
394 read Section 2.2). Therefore, we allow regional climate and socio-economic conditions to vary  
395 independently.

396 As the complete combinatory set of storylines might overwhelm the decision-maker, we use  
397 the scenario-axis technique (van 't Klooster & van Asselt, 2006). We define climate uncertainty  
398 on one axis and socio-economic uncertainty on the other. Two climate storylines are integrated  
399 with two socio-economic scenarios. On each axis, the two most divergent scenarios are chosen  
400 to highlight the spread in outcomes.

## 401 **3 Results**

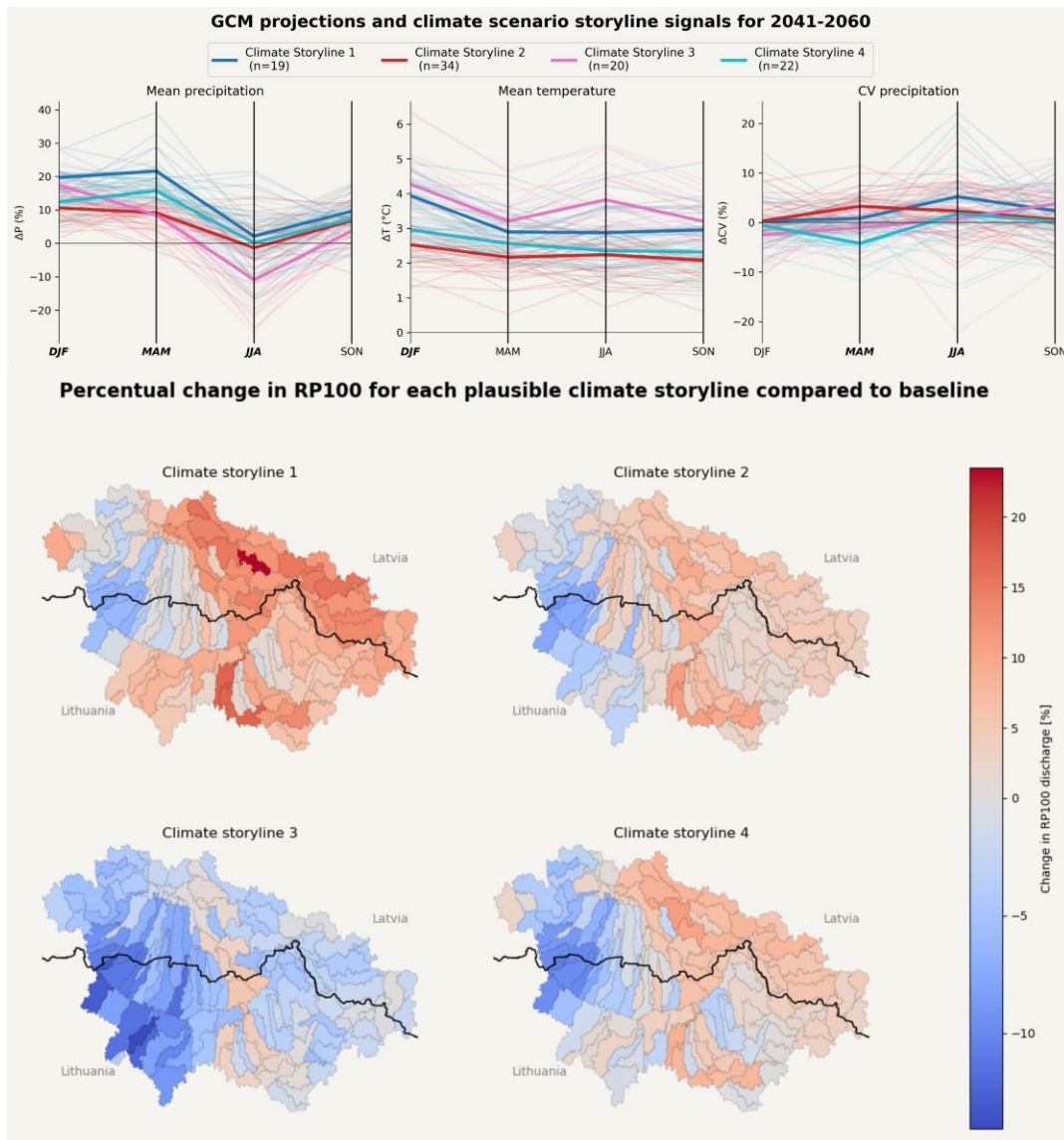
### 402 **3.1 Future discharge changes**

403 After generating various weather time series of future climate scenarios and analysing the  
404 resulting conditional 1/100-year return period discharge changes across CIDs, we find six  
405 unique CIDs most relevant for the eight selected stations in the basin. Three of these are the  
406 average rainfall in winter, spring and summer, causing soil saturation to rise, leading to higher  
407 runoffs. Additionally, changes in the coefficient of variation (CV) of precipitation in spring and  
408 summer are found to be important. Increases in CV correspond to more intense rainfall  
409 patterns, intensifying floods. Lastly, temperature in winter is a driver of discharge change due  
410 to the influence on snow accumulation and melt. While sudden snowmelt is currently a large  
411 driver of floods, this effect decreases when average temperatures rise and snow volume is  
412 reduced. See Appendix A Figure A.2 for the effects of the individual drivers on discharges across  
413 stations.

414 GCM projections are clustered into four climate scenario storylines based on the associated  
415 regional response of the six selected CIDs. For each cluster, the multi-model average climate  
416 signal for the seasonal climate indicators is calculated. Figure 5 plots the storyline signals for  
417 seasonal precipitation, temperature, and precipitation CV changes. Larger changes in rainfall  
418 roughly coincide with larger temperature changes. Climate scenario storylines 1, 2, and 4 show  
419 similar trends with increasing monthly precipitation except in the summer months, where there  
420 is limited change. In contrast, storyline 3 shows less pronounced precipitation changes except  
421 for the summer months, which show a drying trend. For the CV values, we can see a large  
422 variability of potential changes in the full set of GCM signals.

423 Figure 5 also shows changes in the 100-year return period extreme discharge for the different  
424 climate storylines across the basin. Storyline 1 has the largest changes in the region. This is  
425 expected as the storyline is projected to have the most exacerbating changes of relevant CIDs,  
426 such as high increases in precipitation amounts during the winter and spring and increased  
427 rainfall variability in summer. Climate storylines 2 and 4 are similar to storyline 1 but with  
428 smaller changes. In climate storyline 3, many regions experience a decrease in extreme  
429 discharge. This reduction is tied to a combination of CIDs, rainfall decrease in summer and high  
430 winter temperatures, favouring lower flood peaks. Drying in the summer desaturates soils, with  
431 relatively limited recharge in the remaining months and low snow accumulation due to high  
432 temperatures. In general, a similar spatial pattern can be seen across the climate storylines,  
433 where the west of the basin is expected to have lower peak discharges in all climate storylines.  
434 These locations have smaller streams that are particularly sensitive to snow melt-induced

435 extreme discharges. Since all climate storylines indicate a temperature increase, extreme snow  
 436 melt occurs less frequently and less intensely.  
 437

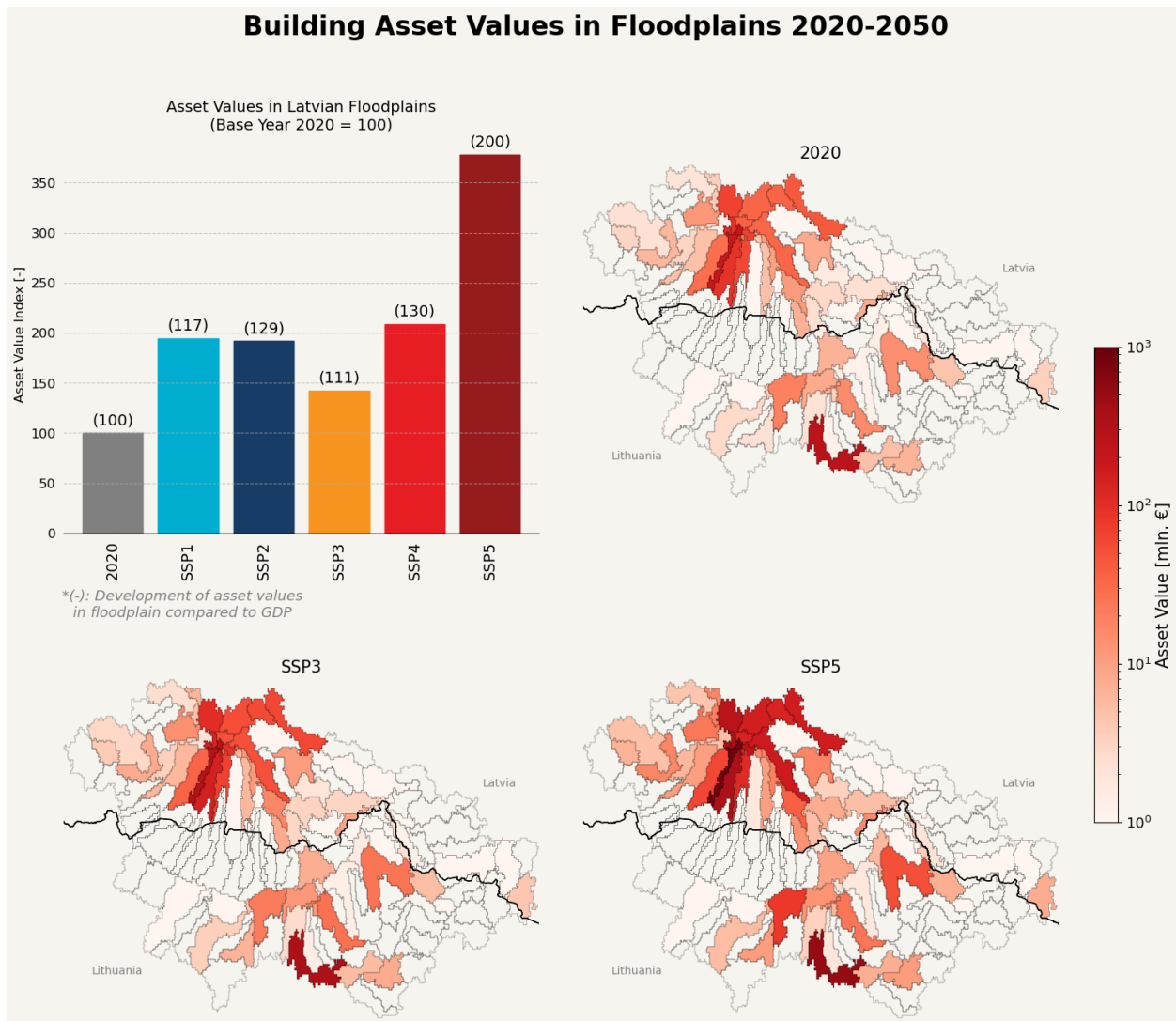


438  
 439 **Figure 5:** The top panel shows seasonal patterns of mean precipitation, temperature and precipitation variability  
 440 for four climate scenario storylines derived to assess ranges in regional discharge response to global warming.  
 441 Thick coloured lines represent the storyline's mean projections. Thin lines represent individual model projections  
 442 colour-coded according to the storyline cluster. In the legend, 'n=#' signifies the number of GCMs assigned to the  
 443 cluster. The bottom panel shows the change in 1/100-year probability discharge across the sub-catchments in the  
 444 basin for each climate storyline.

### 445 3.2 socio-economic trends on exposure

446 The basin aggregated asset value in Latvian floodplains is shown in Figure 6 for each socio-  
 447 economic scenario, together with a spatial distribution of asset values across the basin for

448 selected divergent scenarios. An overall increase in building asset reconstruction value is found,  
 449 especially in the regional economic future inspired by SSP5, where values rise to about 375%  
 450 compared to the original. Also notable is the doubling of floodplain asset values compared to  
 451 GDP in SSP5, indicating an increased value accumulation in floodplains compared to the 2020  
 452 baseline. The largest collection of assets in the floodplain continues to coincide with present-  
 453 day urban centres. These urban centres also develop faster than the surrounding rural areas.  
 454



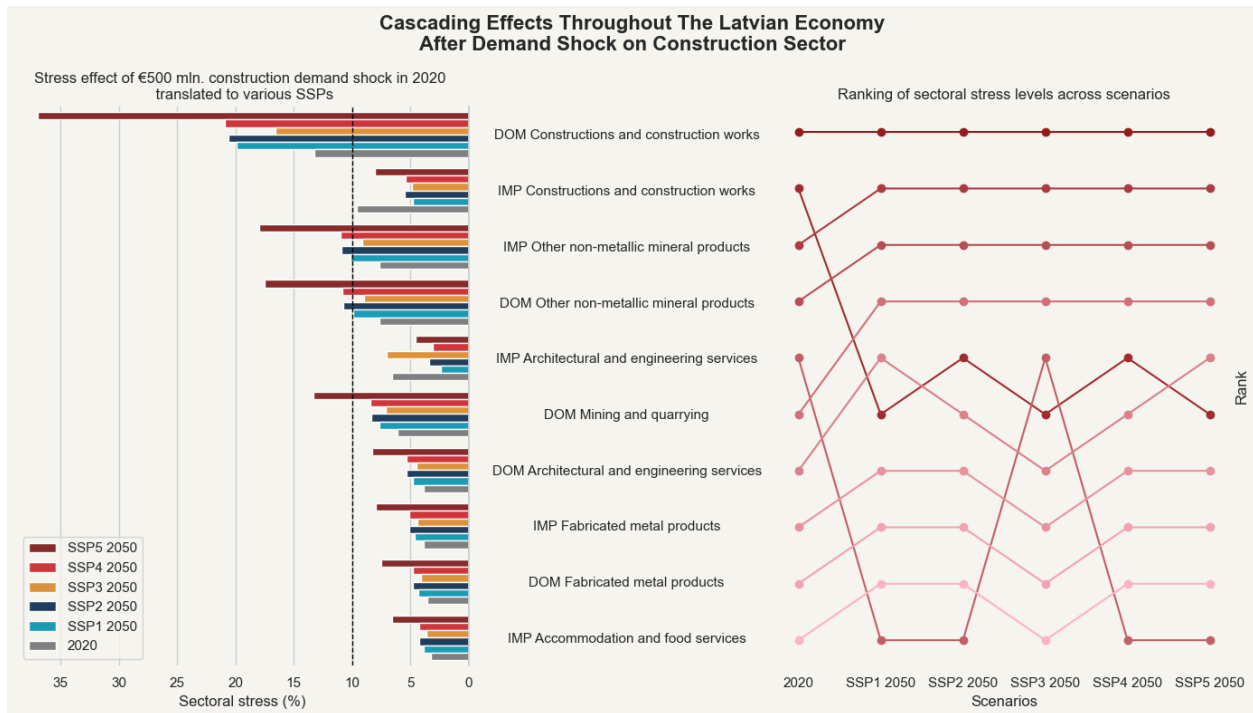
455  
 456 **Figure 6:** Building asset values in floodplain across SSPs relative to base year 2020. The top left shows the  
 457 development of accumulated values in Latvia compared to the base year. In brackets, the asset values in the  
 458 floodplain are compared to the national GDP in the SSP-inspired regional economic future. The remaining plots  
 459 show the spatial development of building asset value for the 2020 baseline and the most divergent future socio-  
 460 economic scenarios.

**461 3.3 Cascading effects**

462 For the various economic scenarios, the Latvian economy experiences varying sectoral stresses  
463 when confronted with a spike in construction demand, as seen in Figure 7. Stress is defined  
464 here as the flood-induced demand compared to the pre-event demand. Sectors closely related  
465 to construction are under the highest stress in the baseline, and in most of these sectors,  
466 stresses rise as asset values in the floodplains increase. At the same time, stresses are  
467 compounded by the in Leimbach et al. (2023) projected shrinking of manufacturing sectors  
468 across all SSP-inspired regional economic futures, leading to higher construction demand  
469 shocks and fewer resources to meet them. Stresses in the construction sector can rise from  
470 about 12% extra workload in the 2020 baseline situation to 36% in SSP5. Many other sectors  
471 can expect a doubling of their stress levels in SSP5 compared to levels in 2020. In their analysis,  
472 Koks & Thissen (2016) assume a production absorption capacity of 10% relative to the pre-  
473 disaster production levels for industries. Using 10% as a stress threshold, our findings show that  
474 when the region is confronted with a 2020 €500 mln. equivalent reconstruction demand shock,  
475 sectors can cross the stress tipping point for some regional economic futures, meaning the  
476 increased demand cannot be absorbed. Socio-economic developments can thus be a key driver  
477 in defining whether sectors will be overwhelmed and unable to meet additional demands  
478 induced by floods.

479 Rankings of those sectors under the most stress also shift. For example, domestic architectural  
480 services experience increased stress, while imports by the same sector decrease in stress. As  
481 more service work is performed domestically, the demand and stresses shift from import  
482 sectors to domestic ones. Meanwhile, the stress ranking of construction imports decreases  
483 because this sector has grown significantly compared to its domestic counterpart; as more  
484 processes are offshored, import sectors become more capable of handling the demand shock,  
485 increasing the capabilities of absorbing increased demands.

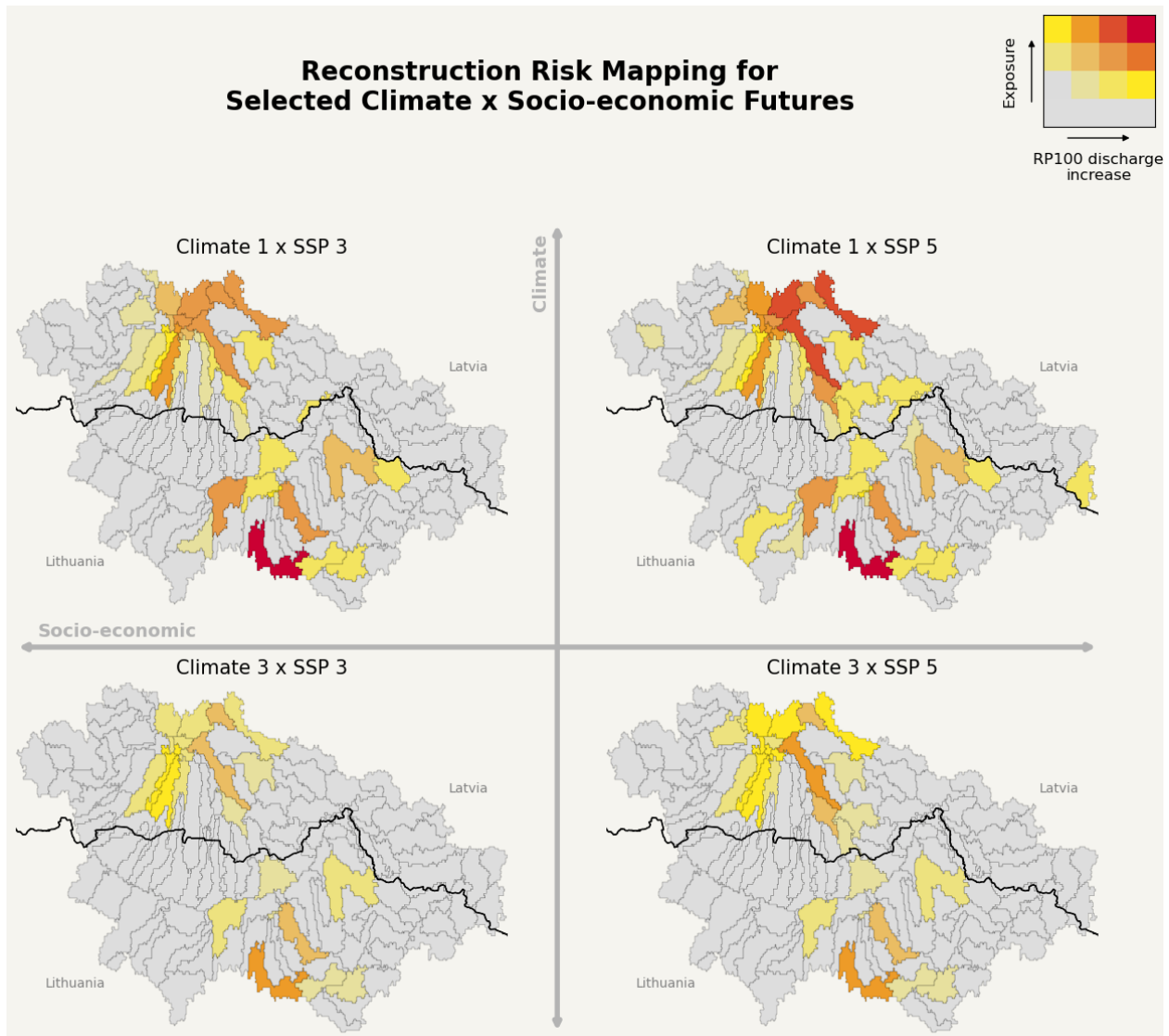
486



487  
 488 **Figure 7:** Sectoral stress levels in response to a €500 million (in 2020 and projected for each SSP) construction  
 489 demand shock across different scenarios, displayed as a bar chart (left) and a bump plot (right). The bar chart  
 490 illustrates the percentual stress levels across scenarios in various sectors due to the shock. The bump plot ranks  
 491 sectors by stress level across scenarios, with the vertical position of each line indicating each sector's rank, with the  
 492 sector under the most stress at the top. Each line is colour-coded from most stress (dark red) to least stress (light  
 493 red) according to 2020 ranks. "DOM" indicates domestic sectors, while "IMP" represents imported products,  
 494 highlighting the distinction between locally produced and imported sectoral impacts.

### 495 3.4 Compounding effects

496 Figure 8 integrates the most divergent socio-economic and climate storylines to detect patterns  
 497 of compounding risk drivers. The underlying data are already shown in Figures 5 and 6.  
 498 Noticeably, entirely new high-risk areas emerge alongside risk intensification in already high-  
 499 risk sub-catchments. The scenario with the highest risk levels is a combination of Climate 1 and  
 500 SSP 5. More asset values are situated in the floodplains due to high urban development, while  
 501 the wetting of the climate causes more antecedent soil moisture, leading to increased  
 502 discharges. The lowest risk scenario is the combination of Climate 3 and SSP 3. In this case, the  
 503 floodplain has low urban development, leading to fewer losses when an event occurs.  
 504 Meanwhile, extreme discharges mainly decrease throughout the region due to reduced  
 505 antecedent soil moisture and snowpack volumes. Although there is significant variability across  
 506 scenarios, sub-catchments that always face relatively high-risk levels can be identified.



507

508 **Figure 8:** Spatial reconstruction risk mapping under selected storylines highlighting potential regional climate and  
 509 socio-economic developments. Each map highlights hazard changes and exposure levels using a bivariate colour  
 510 map, providing a measure of compounding risk drivers.

511 **4 Discussion**

512 **4.1 The consequences of uncertainties and the importance of exploration**

513 Results highlight the importance of using multiple climate storylines to robustly assess future  
 514 discharge extremes. Flood patterns vary significantly across storylines; while some indicate 10%  
 515 regional reductions in the 1-in-100 return period discharge, others indicate increases up to  
 516 20%. The storylines also reveal spatial heterogeneity: in some storylines and regions flood  
 517 preconditions such as snow melt are dampened, whereas other preconditions (such as soil  
 518 moisture volume) are amplified.

519 Projected socio-economic changes can further compound these risks. As exposed asset values  
520 in the Latvian basin almost quadruple compared to the 2020 baseline, sectors are confronted  
521 with heightened flood-induced demand shocks related to reconstruction. Simultaneously, a  
522 trend of declining domestic manufacturing capacity doubles or triples most sectoral stresses  
523 relative to the 2020 baseline. In some scenarios, the demand shock exceeds sectors their  
524 absorptive capacity, amplifying and prolonging indirect impacts (Hallegatte et al., 2024).  
525 Furthermore, increased dependency on imports due to the offshoring of the manufacturing  
526 sectors may create new vulnerabilities to foreign supply disruptions (Ercin et al., 2021).  
527 Conversely, this may lead to enhanced regional resilience through import diversification  
528 (Willner et al., 2018).

529 This methodology is designed to create a diverse yet analytically affordable set of risk scenarios.  
530 To do so, certain choices were made that limited the uncertainty exploration. While our climate  
531 storylines selection method enhances impact exploration compared to emission scenario-based  
532 clustering of GCM projections (Buskop et al., 2024), it reduces the explored impact range  
533 relative to the full ensemble of model outputs. Similarly, averaging discharge change results  
534 across multiple stochastic weather realizations reduced the variability in outcomes. Both steps  
535 involved a trade-off between sampling robustness and exploration. Other aggregation choices  
536 could have been made and is a topic of further discussion in the literature.

#### 537 **4.2 Global projections for the local context**

538 Our methodology uses freely available global data and tools, making it flexible to apply to a  
539 diverse set of regions for which climate risks need to be mapped. Our methodology for  
540 selecting climate scenario storylines could also be applied to other hazards by changing the  
541 CIDs of interest, such as those relevant to drought impacts. Additionally, the projected macro-  
542 economic input-output tables provide versatility to analyse cascading effects arising from  
543 impacts in a variety of sectors. For instance, the preliminary analysis for this study also  
544 addressed agricultural impacts and cascading disruptions within the region. However, for Latvia  
545 these were minor compared to the (in)direct impacts on the reconstruction sector and have  
546 therefore not been considered in detail.

547 The geographical and sectoral flexibility comes with its limitations. Although the risk scoping  
548 was guided by (grey) literature specifically targeting regional issues, the used socio-economic  
549 projections are derived from downscaled global datasets. Consequently, these projections may  
550 not fully capture local socio-economic developments, as global studies do not capture regional  
551 nuances and policies (Blankespoor et al., 2023). Therefore, the accuracy of risk information  
552 from our methodology should be verified with regional stakeholders and adjusted if needed.

553 This study could benefit from localising the global SSPs (Alizadeh et al., 2022; Reimann et al.,  
554 2021) to incorporate policies influencing sectoral changes or add spatial detail to urban  
555 developments. Adding local socio-economic information could further specify direct and  
556 indirect impacts on specific income groups or businesses and/or sectors, as demonstrated in  
557 Bachner et al. (2024). Additionally, with regards to the hazards, local expertise could refine  
558 climate scenario selection by assigning higher weights to CIDs relevant to known high-risk

559 areas, steering clustering of climate projections. Hazard estimation could benefit from spatial  
560 flood modelling using local hydrodynamic models.

### 561 **4.3 Socio-economic and climate developments for impact attribution**

562 In climate science, attribution often refers to how anthropogenic emissions change the  
563 likelihood of extreme meteorological events (Shepherd, 2016; Stott et al., 2016; van  
564 Oldenborgh et al., 2021). However, extreme meteorological events themselves are not always  
565 sufficient to lead to high impacts. These can also occur from coinciding moderate events (van  
566 der Wiel et al., 2020), and flood impacts are often enhanced due to socio-economic risk drivers  
567 (Merz et al., 2021; Steinhausen et al., 2022; Winsemius et al., 2016). Therefore, impact-focused  
568 attribution can help to better understand and quantify risk drivers' contribution to future  
569 climate risks (Mengel et al., 2021). Under particular conditions socio-economic developments,  
570 rather than climate changes, are the main risk drivers (Barnes et al., 2023). Identifying the  
571 'differences that make a difference' enables risk managers to take targeted actions on the most  
572 impactful risk drivers within their control.

573 Our applied methodology aligns well with an impact attribution framework but is not fully  
574 comprehensive. While we analysed how socio-economic changes and how a changing climate  
575 drive risk, we were not able to quantify their comparative effects in the absence of detailed  
576 flood modelling. Future studies could extend our model chain to include flood maps under  
577 climate change, enabling risk attribution to specific drivers.

### 578 **4.4 System boundaries and their effects**

579 As with many studies, the problem scoping and system boundary definition can significantly  
580 influence outcomes and recommendations. Our research confined the problem boundary to  
581 Latvia and specifically focused on the adverse stress effects. Expanding the scope to intra-  
582 regional effects, using a similar economic input-output method could highlight positive spillover  
583 effects as production is shifted to unaffected areas (Middelanis et al., 2022). Even within Latvia,  
584 positive effects can occur. The disaster event might act as an 'opportunity tipping point'  
585 (Haasnoot et al., 2019), opening a window of opportunity to increase adaptation efforts and  
586 'build back better', as seen in New York after Hurricane Sandy (Rosenzweig & Solecki, 2014).  
587 Reconstruction efforts may also boost the local economy. The labour-intensive construction  
588 work might lower unemployment in the aftermath of business destruction while at the same  
589 time having a positive effect on GDP (Vagliasindi & Gorgulu, 2021). However, further extending  
590 the system boundary to include macro-level trends in the region, such as an ageing population,  
591 can further modulate risks and adaptation opportunities. We, therefore, reiterate that setting  
592 the objectives and system boundary remains an important factor in the climate risk analysis.

## 593 **5 Conclusion**

594 Our ability to manage future climate risks is partly determined by our ability to anticipate these  
595 risks. A task which needs to handle uncertainties in both human and natural systems. This  
596 requires a comprehensive but comprehensible package of targeted climate risk information to  
597 allow for informed adaptation decision-making. To this end, we introduced a novel multi-modal

598 methodology targeting flood risk assessment that explores ‘plausibilistic’ future climate risks by  
599 sampling a range of plausible socio-economic developments and climate storylines with  
600 associated conditional discharge probabilities. By integrating meteorological, hydrological, and  
601 socio-economic perspectives, this approach captures the influence of future changes on both  
602 direct impacts and cascading effects in connected multi-sectoral systems.

603 We used this methodology to examine the changes in and effects of discharge extremes in the  
604 transboundary Latvian-Lithuanian Lielupe river basin. As expected, our findings reveal  
605 significant spatial heterogeneity of future discharge extremes within the basin and across  
606 climate scenario storylines as locally relevant CIDs are amplified or dampened depending on  
607 the sampled climate conditions. As a result, the 100-year return period discharge extreme can  
608 deviate -10% to +20% from the baseline depending on the scenario and region. In parallel,  
609 projected asset development in the floodplains and sectoral growth rates indicate an  
610 intensification of impact. Absolute direct impacts can increase by up to 375%, and most sectoral  
611 stress levels double or triple compared to the baseline. These findings highlight substantial  
612 variability in impacts across scenarios, regions and sectors because of developments of  
613 (spatially compounding) risk drivers in the region.

614 This study underscores the importance of a systems perspective to climate risks as both  
615 climatological uncertainties and socio-economic drivers can amplify or attenuate (cascading)  
616 impacts. Our interdisciplinary methodology allows for the identification of particularly  
617 vulnerable regions and sectors across diverse scenarios, offering valuable insights for robust  
618 adaptation planning. By exploring the uncertainty space of risk-inducing trends, key risk areas  
619 and sectors are identified that call for further study. Through our plausibilistic climate impact  
620 storylines, the exploration and understanding of complex risks can be significantly enhanced.  
621 This approach provides comprehensive and targeted regional climate risk information, which is  
622 essential for prioritising adaptation strategies.

## 623 **Acknowledgements**

624 This research has received funding from the European Union’s Horizon Europe – the Framework  
625 Programme for Research and Innovation (CLIMAAX (grant no. 101093864)). We would like to  
626 thank Dace Zandersone and her team at LEGMC for taking the time to discuss the local  
627 situation. Also a word of appreciation goes to Muneta Yokomatsu at IIASA for the insightful  
628 workshop around the analysed topic. We also thank Valeria Di Fant, Doris Vertegaal, Henrique  
629 M.D. Goulart, Anoek van Tilburg, Julius Schlumberger and Daniel Peregrina Gonzalez for their  
630 ideas and input collected during various conversations around the coffee corner.

## 631 **Open Research**

632 The CMIP6 data can be freely obtained through  
633 <https://cds.climate.copernicus.eu/cdsapp#!/dataset/projections-cmip6>. The historical ERA5  
634 data is obtained from [https://cds.climate.copernicus.eu/cdsapp#!/dataset/reanalysis-era5-](https://cds.climate.copernicus.eu/cdsapp#!/dataset/reanalysis-era5-pressure-levels)  
635 [pressure-levels](https://cds.climate.copernicus.eu/cdsapp#!/dataset/reanalysis-era5-pressure-levels). The open-source hydrological model Wflow is accessible here  
636 <https://deltares.github.io/Wflow.jl/>. The projected socio-economic data can be found by

637 following the citations in the text. Implementation of the used weather generator can be found  
638 at <https://github.com/Deltares-research/weathergen>. Analysis code and data used in this study  
639 is published at Zenodo  
640 ([https://zenodo.org/records/14445553?token=eyJhbGciOiJIUzUxMiJ9.eyJpZCI6IjlmZWZhNDAwLWViYjAtNDM4YS1hMDIkdjI2ZGY4MjNmOCIsImRhdGEiOiJ9LCJyYW5kb20iOiI4YmZhMzRmOWI3ZGE2MjRkZWViMDUxOTNjMTA0YWVmNCJ9.WxH5ejVC-TrvHwc7BkiN8\\_L8EjN-1q5\\_vjllQipYedjg0xa7aRmcczmoHQeS4lf4HBfQ91SVXZv7MtBmDfIELQ](https://zenodo.org/records/14445553?token=eyJhbGciOiJIUzUxMiJ9.eyJpZCI6IjlmZWZhNDAwLWViYjAtNDM4YS1hMDIkdjI2ZGY4MjNmOCIsImRhdGEiOiJ9LCJyYW5kb20iOiI4YmZhMzRmOWI3ZGE2MjRkZWViMDUxOTNjMTA0YWVmNCJ9.WxH5ejVC-TrvHwc7BkiN8_L8EjN-1q5_vjllQipYedjg0xa7aRmcczmoHQeS4lf4HBfQ91SVXZv7MtBmDfIELQ)) and on Github  
644 ([https://github.com/TBuskop/spatial and sectoral climate impacts](https://github.com/TBuskop/spatial_and_sectoral_climate_impacts))

## 645 **References**

- 646 Alizadeh, M. R., Adamowski, J., & Inam, A. (2022). Integrated assessment of localized SSP–RCP  
647 narratives for climate change adaptation in coupled human-water systems. *Science of*  
648 *The Total Environment*, 823, 153660. <https://doi.org/10.1016/j.scitotenv.2022.153660>
- 649 Alodah, A., & Seidou, O. (2020). Influence of output size of stochastic weather generators on  
650 common climate and hydrological statistical indices. *Stochastic Environmental Research*  
651 *and Risk Assessment*, 34(7), 993–1021. Scopus. [https://doi.org/10.1007/s00477-020-](https://doi.org/10.1007/s00477-020-01825-w)  
652 [01825-w](https://doi.org/10.1007/s00477-020-01825-w)
- 653 Andrijevic, M., Huppmann, D., Shah, D., Werning, M., & Hooke, D. (n.d.). *SSP Extensions*  
654 *Explorer*. IIASA Scenario Services App. Retrieved 26 September 2024, from [https://ssp-](https://ssp-extensions.apps.ece.iiasa.ac.at/)  
655 [extensions.apps.ece.iiasa.ac.at/](https://ssp-extensions.apps.ece.iiasa.ac.at/)
- 656 Bachner, G., Knittel, N., Poledna, S., Hochrainer-Stigler, S., & Reiter, K. (2024). Revealing indirect  
657 risks in complex socioeconomic systems: A highly detailed multi-model analysis of flood  
658 events in Austria. *Risk Analysis*, 44(1), 229–243. <https://doi.org/10.1111/risa.14144>
- 659 Barnes, C., Faranda, D., Coppola, E., Grazzini, F., Zachariah, M., Lu, C., Kimutai, J., Pinto, I.,  
660 Pereira, C. M., Sengupta, S., Vahlberg, M., Singh, R., Heinrich, D., & Otto, F. (2023).

661 *Limited net role for climate change in heavy spring rainfall in Emilia-Romagna* [Report].

662 <https://doi.org/10.25561/104550>

663 Bednar-Friedl, B., Biesbroek, R., Schmidt, D. N., Alexander, P., Børsheim, K. Y., Carnicer, J.,

664 Georgopoulou, E., Haasnoot, M., Le Cozannet, G., Lionello, P., Lipka, O., Möllmann, C.,

665 Muccione, V., Mustonen, T., Piepenburg, D., & Whitmarsh, L. (2022). Europe. In H.-O.

666 Pörtner, D. C. Roberts, M. M. B. Tignor, E. S. Poloczanska, K. Mintenbeck, A. Alegría, M.

667 Craig, S. Langsdorf, S. Löschke, V. Möller, A. Okem, & B. Rama (Eds.), *Climate Change*

668 *2022: Impacts, Adaptation and Vulnerability. Contribution of Working Group II to the*

669 *Sixth Assessment Report of the Intergovernmental Panel on Climate Change*. Cambridge

670 University Press.

671 [https://www.ipcc.ch/report/ar6/wg2/downloads/report/IPCC\\_AR6\\_WGII\\_Chapter13.pdf](https://www.ipcc.ch/report/ar6/wg2/downloads/report/IPCC_AR6_WGII_Chapter13.pdf)

672 f

673 Blankespoor, B., Dasgupta, S., Wheeler, D., Jeuken, A., van Ginkel, K., Hill, K., & Hirschfeld, D.

674 (2023). Linking sea-level research with local planning and adaptation needs. *Nature*

675 *Climate Change*, 13(8), Article 8. <https://doi.org/10.1038/s41558-023-01749-7>

676 Buskop, F. E., Sperna-Weiland, F., & van den Hurk, B. (2024). Amplifying exploration of regional

677 climate risks: Clustering future projections on regionally relevant impact drivers instead

678 of emission scenarios. *Environmental Research: Climate*. [https://doi.org/10.1088/2752-](https://doi.org/10.1088/2752-5295/ad9f8f)

679 [5295/ad9f8f](https://doi.org/10.1088/2752-5295/ad9f8f)

- 680 Central Statistical Bureau of Latvia. (2023). *Symmetric input-output table at basic prices*.  
681 Statistics Portal. [https://stat.gov.lv/en/statistics-themes/economy/national-](https://stat.gov.lv/en/statistics-themes/economy/national-accounts/tables/iki060-symmetric-input-output-table-basic-prices)  
682 [accounts/tables/iki060-symmetric-input-output-table-basic-prices](https://stat.gov.lv/en/statistics-themes/economy/national-accounts/tables/iki060-symmetric-input-output-table-basic-prices)
- 683 Challinor, A. J., Adger, W. N., Benton, T. G., Conway, D., Joshi, M., & Frame, D. (2018).  
684 Transmission of climate risks across sectors and borders. *Philosophical Transactions of*  
685 *the Royal Society A: Mathematical, Physical and Engineering Sciences*, 376(2121),  
686 20170301. <https://doi.org/10.1098/rsta.2017.0301>
- 687 Chen, G., Li, X., Liu, X., Chen, Y., Liang, X., Leng, J., Xu, X., Liao, W., Qiu, Y., Wu, Q., & Huang, K.  
688 (2020). Global projections of future urban land expansion under shared socioeconomic  
689 pathways. *Nature Communications*, 11(1), 537. [https://doi.org/10.1038/s41467-020-](https://doi.org/10.1038/s41467-020-14386-x)  
690 [14386-x](https://doi.org/10.1038/s41467-020-14386-x)
- 691 Copernicus Climate Change Service. (2021). *CMIP6 predictions underpinning the C3S decadal*  
692 *prediction prototypes* [Dataset]. ECMWF. <https://doi.org/10.24381/CDS.C866074C>
- 693 Dellink, R., Chateau, J., Lanzi, E., & Magné, B. (2017). Long-term economic growth projections in  
694 the Shared Socioeconomic Pathways. *Global Environmental Change*, 42, 200–214.  
695 <https://doi.org/10.1016/j.gloenvcha.2015.06.004>
- 696 Deser, C. (2020). “Certain Uncertainty: The Role of Internal Climate Variability in Projections of  
697 Regional Climate Change and Risk Management”. *Earth's Future*, 8(12), e2020EF001854.  
698 <https://doi.org/10.1029/2020EF001854>

- 699 Dottori, F., Alfieri, L., Bianchi, A., Skoien, J., & Salamon, P. (2022). A new dataset of river flood  
700 hazard maps for Europe and the Mediterranean Basin. *Earth System Science Data*, *14*(4),  
701 1549–1569. <https://doi.org/10.5194/essd-14-1549-2022>
- 702 Dottori, F., Szewczyk, W., Ciscar, J.-C., Zhao, F., Alfieri, L., Hirabayashi, Y., Bianchi, A., Mongelli,  
703 I., Frieler, K., Betts, R. A., & Feyen, L. (2018). Increased human and economic losses from  
704 river flooding with anthropogenic warming. *Nature Climate Change*, *8*(9), 781–786.  
705 <https://doi.org/10.1038/s41558-018-0257-z>
- 706 Eilander, D., Boisgontier, H., Bouaziz, L. J. e, Buitink, J., Couasnon, A., Dalmijn, B., Hegnauer, M.,  
707 Jong, T. de, Loos, S., Marth, I., & van Verseveld, W. (2023). HydroMT: Automated and  
708 reproducible model building and analysis. *Journal of Open Source Software*, *8*(83), 4897.  
709 <https://doi.org/10.21105/joss.04897>
- 710 Ercin, E., Veldkamp, T. I. E., & Hunink, J. (2021). Cross-border climate vulnerabilities of the  
711 European Union to drought. *Nature Communications*, *12*(1), 3322.  
712 <https://doi.org/10.1038/s41467-021-23584-0>
- 713 European Environment Agency. (2024). *European climate risk assessment: Executive summary*.  
714 Publications Office. <https://data.europa.eu/doi/10.2800/204249>
- 715 Eurostat. (2008). *NACE Rev. 2—Statistical classification of economic activities*. Office for Official  
716 Publications of the European Communities.  
717 <https://ec.europa.eu/eurostat/web/products-manuals-and-guidelines/-/ks-ra-07-015>

- 718 Gao, J., & Pesaresi, M. (2021). Downscaling SSP-consistent global spatial urban land projections  
719 from 1/8-degree to 1-km resolution 2000–2100. *Scientific Data*, 8(1), 281.  
720 <https://doi.org/10.1038/s41597-021-01052-0>
- 721 Geurts, P., Ernst, D., & Wehenkel, L. (2006). Extremely randomized trees. *Machine Learning*,  
722 63(1), 3–42. <https://doi.org/10.1007/s10994-006-6226-1>
- 723 Goulart, H. M. D., Benito Lazaro, I., van Garderen, L., van der Wiel, K., Le Bars, D., Koks, E., &  
724 van den Hurk, B. (2024). Compound flood impacts from Hurricane Sandy on New York  
725 City in climate-driven storylines. *Natural Hazards and Earth System Sciences*, 24(1), 29–  
726 45. <https://doi.org/10.5194/nhess-24-29-2024>
- 727 Gutiérrez, J. M., R.G. Jones, G.T. Narisma, L.M. Alves, M. Amjad, I.V. Gorodetskaya, M. Grose,  
728 N.A.B. Klutse, S. Krakovska, J. Li, D. Martínez-Castro, L.O. Mearns, S.H. Mernild, T. Ngo-  
729 Duc, B. van den Hurk, & J.-H. Yoon. (2021). Atlas. In *Climate Change 2021: The Physical  
730 Science Basis. Contribution of Working Group I to the Sixth Assessment Report of the  
731 Intergovernmental Panel on Climate Change* (pp. 1927–2058).  
732 <https://doi.org/10.1017/9781009157896.021>
- 733 Haasnoot, M., Warren, A., & Kwakkel, J. H. (2019). Dynamic Adaptive Policy Pathways (DAPP). In  
734 V. A. W. J. Marchau, W. E. Walker, P. J. T. M. Bloemen, & S. W. Popper (Eds.), *Decision  
735 Making under Deep Uncertainty: From Theory to Practice* (pp. 71–92). Springer  
736 International Publishing. [https://doi.org/10.1007/978-3-030-05252-2\\_4](https://doi.org/10.1007/978-3-030-05252-2_4)

- 737 Haklay, M., & Weber, P. (2008). OpenStreetMap: User-Generated Street Maps. *IEEE Pervasive*  
738 *Computing*, 7(4), 12–18. IEEE Pervasive Computing.  
739 <https://doi.org/10.1109/MPRV.2008.80>
- 740 Hallegatte, S., Jooste, C., & Mclsaac, F. (2024). Modeling the macroeconomic consequences of  
741 natural disasters: Capital stock, recovery dynamics, and monetary policy. *Economic*  
742 *Modelling*, 139, 106787. <https://doi.org/10.1016/j.econmod.2024.106787>
- 743 Hawkins, E., & Sutton, R. (2011). The potential to narrow uncertainty in projections of regional  
744 precipitation change. *Climate Dynamics*, 37(1), 407–418.  
745 <https://doi.org/10.1007/s00382-010-0810-6>
- 746 Hersbach, H., Bell, B., Berrisford, P., Biavati, G., Horányi, A., Sabater, J. M., Nicolas, J., Peubey,  
747 C., Radu, R., Rozum, I., Schepers, D., Simmons, A., Soci, C., Dee, D., & Thépaut, J.-N.  
748 (2023). *ERA5 hourly data on pressure levels from 1940 to present* [Dataset]. Copernicus  
749 Climate Change Service (C3S) Climate Data Store (CDS).  
750 <https://doi.org/10.24381/cds.bd0915c6>
- 751 Hochrainer-Stigler, S., Šakić Trogrlić, R., Reiter, K., Ward, P. J., Ruiter, M. C. de, Duncan, M. J.,  
752 Torresan, S., Ciurean, R., Mysiak, J., Stuparu, D., & Gottardo, S. (2023). Towards a  
753 framework for systemic multi-hazard and multi-risk assessment and management.  
754 *iScience*, 106736. <https://doi.org/10.1016/j.isci.2023.106736>
- 755 Huizinga, J., de Moel, H., & Szewczyk, W. (2016). *Global flood depth-damage functions:*  
756 *Methodology and the database with guidelines*. Publications Office of the European  
757 Union. <https://data.europa.eu/doi/10.2760/16510>

- 758 Kirchoff, C. J., Lemos, M. C., & Dessai, S. (2013). Actionable Knowledge for Environmental  
759 Decision Making: Broadening the Usability of Climate Science. *Annual Review of*  
760 *Environment and Resources*, 38(Volume 38, 2013), 393–414.  
761 <https://doi.org/10.1146/annurev-environ-022112-112828>
- 762 Koks, E. E., & Thissen, M. (2016). A Multiregional Impact Assessment Model for disaster  
763 analysis. *Economic Systems Research*, 28(4), 429–449.  
764 <https://doi.org/10.1080/09535314.2016.1232701>
- 765 Lawrence, J., Blackett, P., & Cradock-Henry, N. A. (2020). Cascading climate change impacts and  
766 implications. *Climate Risk Management*, 29, 100234.  
767 <https://doi.org/10.1016/j.crm.2020.100234>
- 768 Lehner, B., & Grill, G. (2013). Global river hydrography and network routing: Baseline data and  
769 new approaches to study the world's large river systems. *Hydrological Processes*, 27(15),  
770 2171–2186. <https://doi.org/10.1002/hyp.9740>
- 771 Lehner, F., Deser, C., Maher, N., Marotzke, J., Fischer, E. M., Brunner, L., Knutti, R., & Hawkins,  
772 E. (2020). Partitioning climate projection uncertainty with multiple large ensembles and  
773 CMIP5/6. *Earth System Dynamics*, 11(2), 491–508. [https://doi.org/10.5194/esd-11-491-](https://doi.org/10.5194/esd-11-491-2020)  
774 2020
- 775 Leimbach, M., Marcolino, M., & Koch, J. (2023). Structural change scenarios within the SSP  
776 framework. *Futures*, 150, 103156. <https://doi.org/10.1016/j.futures.2023.103156>

- 777 Lemos, M. C., Kirchhoff, C. J., & Ramprasad, V. (2012). Narrowing the climate information  
778 usability gap. *Nature Climate Change*, 2(11), 789–794.  
779 <https://doi.org/10.1038/nclimate1614>
- 780 Lempert, R. J. (2013). Scenarios that illuminate vulnerabilities and robust responses. *Climatic*  
781 *Change*, 117(4), 627–646. <https://doi.org/10.1007/s10584-012-0574-6>
- 782 Lempert, R. J., Popper, S. W., & Bankes, S. C. (2003). *Shaping the Next One Hundred Years: New*  
783 *Methods for Quantitative, Long-Term Policy Analysis*. RAND Corporation.  
784 [https://www.rand.org/pubs/monograph\\_reports/MR1626.html](https://www.rand.org/pubs/monograph_reports/MR1626.html)
- 785 Leontief, W. W. (1936). Quantitative Input and Output Relations in the Economic Systems of the  
786 United States. *The Review of Economics and Statistics*, 18(3), 105–125.  
787 <https://doi.org/10.2307/1927837>
- 788 Levermann, A. (2014). Climate economics: Make supply chains climate-smart. *Nature*,  
789 506(7486), 27–29. <https://doi.org/10.1038/506027a>
- 790 Liné, A., Cassou, C., Msadek, R., & Parey, S. (2024). Modulation of Northern Europe near-term  
791 anthropogenic warming and wettening assessed through internal variability storylines.  
792 *Npj Climate and Atmospheric Science*, 7(1), 1–14. [https://doi.org/10.1038/s41612-024-](https://doi.org/10.1038/s41612-024-00759-2)  
793 [00759-2](https://doi.org/10.1038/s41612-024-00759-2)
- 794 Linnerooth-Bayer, J., & Hochrainer-Stigler, S. (2015). Financial instruments for disaster risk  
795 management and climate change adaptation. *Climatic Change*, 133(1), 85–100.  
796 <https://doi.org/10.1007/s10584-013-1035-6>

- 797 Mechler, R., Bouwer, L. M., Linnerooth-Bayer, J., Hochrainer-Stigler, S., Aerts, J. C. J. H.,  
798 Surminski, S., & Williges, K. (2014). Managing unnatural disaster risk from climate  
799 extremes. *Nature Climate Change*, 4(4), 235–237. <https://doi.org/10.1038/nclimate2137>
- 800 Mengel, M., Treu, S., Lange, S., & Frieler, K. (2021). ATTRICI v1.1 – counterfactual climate for  
801 impact attribution. *Geoscientific Model Development*, 14(8), 5269–5284.  
802 <https://doi.org/10.5194/gmd-14-5269-2021>
- 803 Merz, B., Blöschl, G., Vorogushyn, S., Dottori, F., Aerts, J. C. J. H., Bates, P., Bertola, M., Kemter,  
804 M., Kreibich, H., Lall, U., & Macdonald, E. (2021). Causes, impacts and patterns of  
805 disastrous river floods. *Nature Reviews Earth & Environment*, 2(9), 592–609.  
806 <https://doi.org/10.1038/s43017-021-00195-3>
- 807 Middelanis, R., Willner, S. N., Otto, C., Kuhla, K., Quante, L., & Levermann, A. (2021). Wave-like  
808 global economic ripple response to Hurricane Sandy. *Environmental Research Letters*,  
809 16(12), 124049. <https://doi.org/10.1088/1748-9326/ac39c0>
- 810 Middelanis, R., Willner, S. N., Otto, C., & Levermann, A. (2022). Economic losses from hurricanes  
811 cannot be nationally offset under unabated warming. *Environmental Research Letters*,  
812 17(10), 104013. <https://doi.org/10.1088/1748-9326/ac90d8>
- 813 Miller, R. E., & Blair, P. D. (2009). *Input-Output Analysis: Foundations and Extensions* (2nd ed.).  
814 Cambridge University Press. <https://doi.org/10.1017/CBO9780511626982>
- 815 Ministry of Environmental Protection and Regional Development. (2019). *LATVIAN NATIONAL*  
816 *PLAN FOR ADAPTATION TO CLIMATE CHANGE UNTIL 2030*.  
817 <https://likumi.lv/doc.php?id=308330>

- 818 Mora, C., Frazier, A. G., Longman, R. J., Dacks, R. S., Walton, M. M., Tong, E. J., Sanchez, J. J.,  
819 Kaiser, L. R., Stender, Y. O., Anderson, J. M., Ambrosino, C. M., Fernandez-Silva, I.,  
820 Giuseffi, L. M., & Giambelluca, T. W. (2013). The projected timing of climate departure  
821 from recent variability. *Nature*, *502*(7470), Article 7470.  
822 <https://doi.org/10.1038/nature12540>
- 823 O'Neill, B. C., Kriegler, E., Ebi, K. L., Kemp-Benedict, E., Riahi, K., Rothman, D. S., van Ruijven, B.  
824 J., van Vuuren, D. P., Birkmann, J., Kok, K., Levy, M., & Solecki, W. (2017). The roads  
825 ahead: Narratives for shared socioeconomic pathways describing world futures in the  
826 21st century. *Global Environmental Change*, *42*, 169–180.  
827 <https://doi.org/10.1016/j.gloenvcha.2015.01.004>
- 828 O'Neill, B. C., Kriegler, E., Riahi, K., Ebi, K. L., Hallegatte, S., Carter, T. R., Mathur, R., & van  
829 Vuuren, D. P. (2014). A new scenario framework for climate change research: The  
830 concept of shared socioeconomic pathways. *Climatic Change*, *122*(3), 387–400.  
831 <https://doi.org/10.1007/s10584-013-0905-2>
- 832 Pigaiani, C., & Batista e Silva, F. (2021). *The LUISA base map 2018: A geospatial data fusion*  
833 *approach to increase the detail of European land use/land cover data*. Publications  
834 Office of the European Union. <https://data.europa.eu/doi/10.2760/503006>
- 835 Reimann, L., Vollstedt, B., Koerth, J., Tsakiris, M., Beer, M., & Vafeidis, A. T. (2021). Extending  
836 the Shared Socioeconomic Pathways (SSPs) to support local adaptation planning—A  
837 climate service for Flensburg, Germany. *Futures*, *127*, 102691.  
838 <https://doi.org/10.1016/j.futures.2020.102691>

- 839 Rosenzweig, C., & Solecki, W. (2014). Hurricane Sandy and adaptation pathways in New York:  
840 Lessons from a first-responder city. *Global Environmental Change*, 28, 395–408.  
841 <https://doi.org/10.1016/j.gloenvcha.2014.05.003>
- 842 Shepherd, T. G. (2016). A Common Framework for Approaches to Extreme Event Attribution.  
843 *Current Climate Change Reports*, 2(1), 28–38. [https://doi.org/10.1007/s40641-016-](https://doi.org/10.1007/s40641-016-0033-y)  
844 [0033-y](https://doi.org/10.1007/s40641-016-0033-y)
- 845 Shepherd, T. G. (2019). Storyline approach to the construction of regional climate change  
846 information. *Proceedings of the Royal Society A: Mathematical, Physical and Engineering*  
847 *Sciences*, 475(2225), 20190013. <https://doi.org/10.1098/rspa.2019.0013>
- 848 Shepherd, T. G., Boyd, E., Calel, R. A., Chapman, S. C., Dessai, S., Dima-West, I. M., Fowler, H. J.,  
849 James, R., Maraun, D., Martius, O., Senior, C. A., Sobel, A. H., Stainforth, D. A., Tett, S. F.  
850 B., Trenberth, K. E., van den Hurk, B. J. J. M., Watkins, N. W., Wilby, R. L., & Zenghelis, D.  
851 A. (2018). Storylines: An alternative approach to representing uncertainty in physical  
852 aspects of climate change. *Climatic Change*, 151(3), 555–571.  
853 <https://doi.org/10.1007/s10584-018-2317-9>
- 854 Sieg, T., Schinko, T., Vogel, K., Mechler, R., Merz, B., & Kreibich, H. (2019). Integrated  
855 assessment of short-term direct and indirect economic flood impacts including  
856 uncertainty quantification. *PLOS ONE*, 14(4), e0212932.  
857 <https://doi.org/10.1371/journal.pone.0212932>

- 858 Sillmann, J., Shepherd, T. G., van den Hurk, B., Hazeleger, W., Martius, O., Slingo, J., &  
859 Zscheischler, J. (2021). Event-Based Storylines to Address Climate Risk. *Earth's Future*,  
860 9(2), e2020EF001783. <https://doi.org/10.1029/2020EF001783>
- 861 Steinhausen, M., Paprotny, D., Dottori, F., Sairam, N., Mentaschi, L., Alfieri, L., Lüdtkke, S.,  
862 Kreibich, H., & Schröter, K. (2022). Drivers of future fluvial flood risk change for  
863 residential buildings in Europe. *Global Environmental Change*, 76, 102559.  
864 <https://doi.org/10.1016/j.gloenvcha.2022.102559>
- 865 Steinschneider, S., & Brown, C. (2013). A semiparametric multivariate, multisite weather  
866 generator with low-frequency variability for use in climate risk assessments. *Water*  
867 *Resources Research*, 49(11), 7205–7220. <https://doi.org/10.1002/wrcr.20528>
- 868 Stott, P. A., Christidis, N., Otto, F. E. L., Sun, Y., Vanderlinden, J.-P., van Oldenborgh, G. J.,  
869 Vautard, R., von Storch, H., Walton, P., Yiou, P., & Zwiers, F. W. (2016). Attribution of  
870 extreme weather and climate-related events. *WIREs Climate Change*, 7(1), 23–41.  
871 <https://doi.org/10.1002/wcc.380>
- 872 Tukker, A., Bulavskaya, T., Giljum, S., de Koning, A., Lutter, S., Simas, M., Stadler, K., & Wood, R.  
873 (2016). Environmental and resource footprints in a global context: Europe's structural  
874 deficit in resource endowments. *Global Environmental Change*, 40, 171–181.  
875 <https://doi.org/10.1016/j.gloenvcha.2016.07.002>
- 876 Vagliasindi, M., & Gorgulu, N. (2021). *What have we Learned about the Effectiveness of*  
877 *Infrastructure Investment as a Fiscal Stimulus? A Literature Review* (Policy Research  
878 Working Papers). The World Bank. <https://doi.org/10.1596/1813-9450-9796>

- 879 van den Hurk, B. J. J. M. (2022). Impact-Oriented Climate Information Selection. *Springer*  
880 *Climate*, 27–32. [https://doi.org/10.1007/978-3-030-86211-4\\_4](https://doi.org/10.1007/978-3-030-86211-4_4)
- 881 van den Hurk, B. J. J. M., Baldissera Pacchetti, M., Boere, E., Ciullo, A., Coulter, L., Dessai, S.,  
882 Ercin, E., Goulart, H. M. D., Hamed, R., Hochrainer-Stigler, S., Koks, E., Kubiczek, P.,  
883 Levermann, A., Mechler, R., van Meersbergen, M., Mester, B., Middelani, R.,  
884 Minderhoud, K., Mysiak, J., ... Witpas, K. (2023). Climate impact storylines for assessing  
885 socio-economic responses to remote events. *Climate Risk Management*, 40, 100500.  
886 <https://doi.org/10.1016/j.crm.2023.100500>
- 887 van der Wiel, K., Beersma, J., van den Brink, H., Krikken, F., Selten, F., Severijns, C., Sterl, A., van  
888 Meijgaard, E., Reerink, T., & van Dorland, R. (2024). KNMI'23 Climate Scenarios for the  
889 Netherlands: Storyline Scenarios of Regional Climate Change. *Earth's Future*, 12(2),  
890 e2023EF003983. <https://doi.org/10.1029/2023EF003983>
- 891 van der Wiel, K., Selten, F. M., Bintanja, R., Blackport, R., & Screen, J. A. (2020). Ensemble  
892 climate-impact modelling: Extreme impacts from moderate meteorological conditions.  
893 *Environmental Research Letters*, 15(3), 034050. [https://doi.org/10.1088/1748-](https://doi.org/10.1088/1748-9326/ab7668)  
894 [9326/ab7668](https://doi.org/10.1088/1748-9326/ab7668)
- 895 van Oldenborgh, G. J., van der Wiel, K., Kew, S., Philip, S., Otto, F., Vautard, R., King, A., Lott, F.,  
896 Arrighi, J., Singh, R., & van Aalst, M. (2021). Pathways and pitfalls in extreme event  
897 attribution. *Climatic Change*, 166(1), 13. <https://doi.org/10.1007/s10584-021-03071-7>
- 898 van 't Klooster, S. A., & van Asselt, M. B. A. (2006). Practising the scenario-axes technique.  
899 *Futures*, 38(1), 15–30. <https://doi.org/10.1016/j.futures.2005.04.019>

- 900 van Verseveld, W., Weerts, A. H., Visser, M., Buitink, J., Imhoff, R. O., Boisgontier, H., Bouaziz,  
901 L., Eilander, D., Hegnauer, M., ten Velden, C., & Russell, B. (2024). Wflow\_sbm v0.7.3, a  
902 spatially distributed hydrological model: From global data to local applications.  
903 *Geoscientific Model Development*, 17(8), 3199–3234. [https://doi.org/10.5194/gmd-17-](https://doi.org/10.5194/gmd-17-3199-2024)  
904 3199-2024
- 905 van Vuuren, D. P., Edmonds, J., Kainuma, M., Riahi, K., Thomson, A., Hibbard, K., Hurtt, G. C.,  
906 Kram, T., Krey, V., Lamarque, J.-F., Masui, T., Meinshausen, M., Nakicenovic, N., Smith, S.  
907 J., & Rose, S. K. (2011). The representative concentration pathways: An overview.  
908 *Climatic Change*, 109(1), 5. <https://doi.org/10.1007/s10584-011-0148-z>
- 909 van Vuuren, D. P., Kriegler, E., O'Neill, B. C., Ebi, K. L., Riahi, K., Carter, T. R., Edmonds, J.,  
910 Hallegatte, S., Kram, T., Mathur, R., & Winkler, H. (2014). A new scenario framework for  
911 Climate Change Research: Scenario matrix architecture. *Climatic Change*, 122(3), 373–  
912 386. <https://doi.org/10.1007/s10584-013-0906-1>
- 913 Wang, T., & Sun, F. (2022). Global gridded GDP data set consistent with the shared  
914 socioeconomic pathways. *Scientific Data*, 9(1), 221. [https://doi.org/10.1038/s41597-](https://doi.org/10.1038/s41597-022-01300-x)  
915 022-01300-x
- 916 Ward, P. J., Winsemius, H. C., Kuzma, S., Bierkens, M. F., Bouwman, A., De Moel, H., Loaiza, A.  
917 D., Eilander, D., Englhardt, J., Erkens, G., & others. (2020). Aqueduct floods  
918 methodology. *World Resources Institute*, 1–28.
- 919 Wilby, R. L., & Dessai, S. (2010). Robust adaptation to climate change. *Weather*, 65(7), 180–185.  
920 <https://doi.org/10.1002/wea.543>

921 Willner, S. N., Otto, C., & Levermann, A. (2018). Global economic response to river floods.

922 *Nature Climate Change*, 8(7), 594–598. <https://doi.org/10.1038/s41558-018-0173-2>

923 Winsemius, H. C., Aerts, J. C. J. H., van Beek, L. P. H., Bierkens, M. F. P., Bouwman, A., Jongman,

924 B., Kwadijk, J. C. J., Ligtoet, W., Lucas, P. L., van Vuuren, D. P., & Ward, P. J. (2016).

925 Global drivers of future river flood risk. *Nature Climate Change*, 6(4), 381–385.

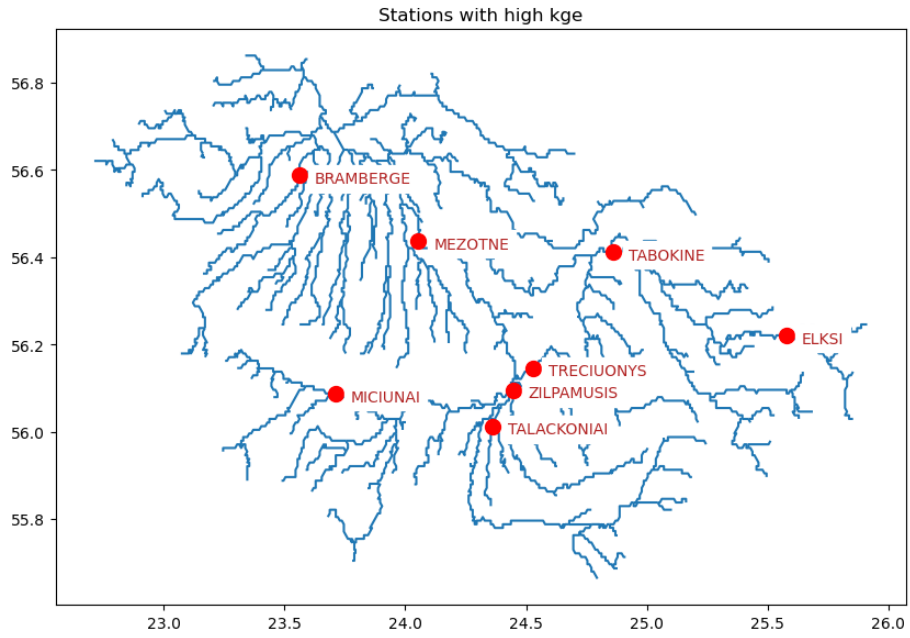
926 <https://doi.org/10.1038/nclimate2893>

927 Appendix A: Obtaining Relevant Climate Impact Drivers

928 **Table A.1:** Table of used models and SSPs in the 2041-2060 timeframe. Model data extracted from Copernicus Data  
929 Store (Copernicus Climate Change Service, 2021)

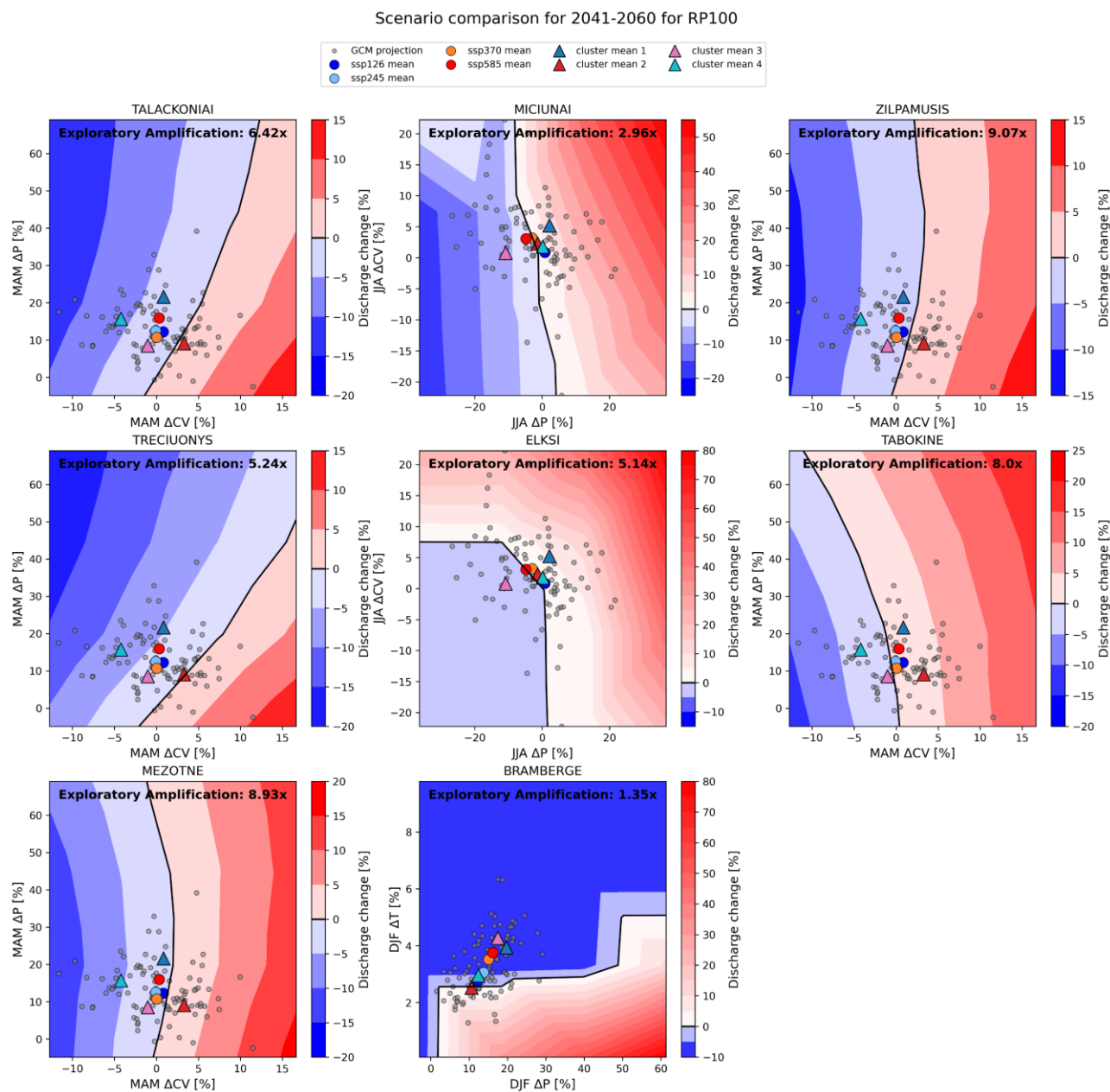
Model Name	SSP1-2.6	SSP2-4.5	SSP3-7.0	SSP5-8.5
ACCESS-CM2	✓	✓	✓	✓
BCC-CSM2-MR	✓	✓	✓	✓
CanESM5	✓			✓
CESM2	✓	✓	✓	✓
CESM2-WACCM			✓	✓
CMCC-CM2-SR5		✓	✓	✓
CMCC-ESM2	✓	✓		✓
CNRM-CM6-1	✓	✓	✓	✓
CNRM-CM6-1-HR	✓			✓
CNRM-ESM2-1	✓	✓	✓	✓
EC-Earth3-AerChem			✓	
EC-Earth3-CC		✓		✓

FGOALS-g3	✓	✓	✓	✓
GFDL-ESM4	✓	✓	✓	✓
HadGEM3-GC31-LL	✓	✓		✓
HadGEM3-GC31-MM	✓			✓
IITM-ESM	✓	✓	✓	✓
INM-CM4-8	✓	✓	✓	✓
INM-CM5-0	✓	✓	✓	✓
IPSL-CM5A2-INCA	✓		✓	
IPSL-CM6A-LR	✓	✓	✓	✓
KACE-1.0-G	✓	✓	✓	✓
KIOST-ESM	✓	✓		
MIROC-ES2L	✓	✓	✓	✓
MIROC6	✓	✓	✓	✓
MPI-ESM1-2-LR	✓	✓	✓	✓
MRI-ESM2-0	✓	✓	✓	✓
NESM3		✓		✓
NorESM2-MM	✓	✓	✓	✓
TAI-ESM1				✓
Count	24	23	21	27



930  
931  
932

**Figure A.1:** A map of the Lielupe basin rivers (in blue) with stations in red with Kling-Gupta Efficiency  $\geq 0.5$  and thus considered in the Climatic Impact driver clustering. The names of the stations are annotated in red.



933  
 934 **Figure A.2:** Impact response for the 2041-2060 timeframe for various stations in the basin and their top two climate  
 935 features of importance. The axis labels represent seasonal changes for December-January-February (DJF), March-  
 936 April-May (MAM), June-July-August (JJA), and September-October-November (SON). For selected seasons, the  
 937 changes in average temperature ( $\Delta T$ ), average precipitation ( $\Delta P$ ) and coefficient of variation ( $\Delta CV$ ) of that  
 938 precipitation are shown. The background hue indicates the discharge change for that return period at any  
 939 combination of the selected climate features. Each grey point represents an individual GCM model projection for  
 940 SSP126, SSP245, SSP370 and SSP585. The coloured circles represent the SSP model means, and coloured triangles  
 941 represent the model means of the different clusters. The exploratory amplification for each station is provided.

## 942 **Appendix B: Projecting Input-Output Tables**

943 This appendix details the projection process of national input-output tables according to socio-  
 944 economic trends and sectoral shifts in SSPs. First, the 2020 national input-output table was  
 945 retrieved from the Latvian statistics portal. This table includes 64 sectors corresponding to the  
 946 NACE64 nomenclature used in the European Union (Eurostat, 2008). Since the projections in  
 947 Leimbach et al. (2023) only cover the aggregate NACE3 sectors, the NACE64 sectors are  
 948 aggregated into the NACE3 sectors: Agriculture, Manufacturing and Services. Contribution  
 949 ratios of sectors within each NACE3 group are kept as is, since more granular sectoral change  
 950 information is not available.

951 The projection process starts by multiplying the 2020 national value added by the projected  
 952 GDP growth in 2050, shown in Figure 4 of the main text. Next, the value added is allocated  
 953 among the three aggregate sectors according to the 2050 projection, providing an estimate of  
 954 each sector's size in 2050 for an SSP.

$$VA_{s,SSP}^{2050} = \alpha_{s,SSP}^{2050} * VA^{2020} * g_{SSP}^{2050}$$

955 Where:

956  $VA_{s,SSP}^{2050}$ : projected value added of NACE3 sector  $s$  in 2050 for an SSP scenario

957  $\alpha_{s,SSP}^{2050}$ : projected sectoral contribution share of NACE3 sector  $s$  in 2050 for an SSP scenario

958  $VA^{2020}$ : total value added in the economy in 2020

959  $g_{SSP}^{2050}$ : growth value of GDP in 2050 for an SSP scenario

960 To maintain a detailed sectoral analysis, the value added of each NACE3 sector is disaggregated  
 961 to the original NACE64 sectors using 2020 value-added contributions ratios within the  
 962 aggregate sector. This proportional allocation assumes that internal distribution within a NACE3  
 963 sector does not change from the base year. Using the updated value added for each sector, the  
 964 required input goods from the NACE64 sectors are calculated based on the 2020 ratio of input  
 965 units per unit of value added.

966

$$VA_{i,SSP}^{2050} = VA_{s,SSP}^{2050} * \frac{VA_i^{2020}}{VA_s^{2020}}$$

967 Where:

968  $VA_{i,SSP}^{2050}$ : projected value added of NACE64 sector  $i$  in 2050 for an SSP scenario

969  $VA_{s,SSP}^{2050}$ : projected value added of NACE3 sector  $s$  in 2050 for an SSP scenario

970  $VA_i^{2020}$ : value added of NACE64 sector  $i$  in 2020

971  $VA_s^{2020}$ : value added of NACE3 sector  $s$  in 2020

972

$$Input_{i \leftarrow j,SSP}^{2050} = VA_{i,SSP}^{2050} * \frac{Input_{i \leftarrow j}^{2020}}{VA_i^{2020}}$$

973 Where:

974  $Input_{i \leftarrow j, SSP}^{2050}$ : input required from sector  $j$  for sector  $i$  in 2050 for an SSP scenario

975  $Input_{i \leftarrow j}^{2020}$ : input required from sector  $j$  for sector  $i$  in 2020

976  $VA_{i, SSP}^{2050}$ : projected value added of NACE64 sector  $i$  in 2050 for an SSP scenario

977  $VA_i^{2020}$ : value added of NACE64 sector  $i$  in 2020

978 Meanwhile, the final demands for each sector's output, sectoral goods not used as  
 979 intermediate inputs for other sectors (such as household consumption or government  
 980 spending), are scaled with overall national GDP increases to anticipate increases in  
 981 consumption patterns.

$$FD_{i, SSP}^{2050} = FD_i^{2020} * g_{SSP}^{2050}$$

982 Where:

983  $FD_{i, SSP}^{2050}$ : final demand for sector  $i$  in 2050 for an SSP scenario

984  $FD_i^{2020}$ : final demand for sector  $i$  in 2020

985  $g_{SSP}^{2050}$ : growth value of GDP in 2050 for an SSP scenario

986 These calculations may cause growing sectors to demand inputs from shrinking domestic  
 987 sectors, which may be unable to meet those demands. Conversely, some sectors may produce  
 988 more than local demand requires. This creates an imbalance between a sector's inputs and  
 989 outputs. However, a fundamental notion in the IO framework is that each sector's inputs and  
 990 outputs must balance. This balance ensures that all produced goods are allocated and input  
 991 goods are sourced appropriately in the accounting. To balance the table we introduce  
 992 additional imports and exports for the mentioned cases.

$$X_i^{2050} = VA_{i, SSP}^{2050} + \sum_j Input_{i \leftarrow j, SSP}^{2050}$$

993 Where:

994  $X_i^{2050}$ : total output of sector  $i$

995  $Input_{i \leftarrow j, SSP}^{2050}$ : input required from sector  $j$  for sector  $i$  in 2050 for an SSP scenario

996  $VA_{i, SSP}^{2050}$ : projected value added of sector  $i$  in 2050 for an SSP scenario

997

$$D_{i, SSP}^{2050} = FD_{i, SSP}^{2050} + \sum_j Input_{j \leftarrow i, SSP}^{2050}$$

998 Where:

999  $D_{i, SSP}^{2050}$ : total demand of sector  $i$

1000  $FD_{i, SSP}^{2050}$ : final demand for sector  $i$  in 2050 for an SSP scenario

1001  $Input_{j \leftarrow i, SSP}^{2050}$ : input required by sector  $j$  from sector  $i$  in 2050 for an SSP scenario

1002 In the calculus, the need for exports or imports is determined by subtracting the total inputs  
 1003 into a sector from the total output needed from that sector. The resulting value of extra  
 1004 imports or exports needed are distributed according to usage shares, sectors using most of a

1005 sector's outputs, import most. If local production exceeds local consumption, imports of  
 1006 domestic sectors that require the specific local goods are reduced to zero, and the remaining  
 1007 goods are added to a producing sector's final demand as exports. This process ensures that  
 1008 projected inputs and outputs are in balance.

$$NP_{i,SSP}^{2050} = X_{i,SSP}^{2050} - D_{i,SSP}^{2050}$$

1009 Where:

1010  $NP_{i,SSP}^{2050}$ : net production sector  $i$  in 2050 for an SSP scenario

1011  $X_i^{2050}$ : total output of sector  $i$  in 2050 for an SSP scenario

1012  $D_i^{2050}$ : total demand of sector  $i$  in 2050 for an SSP scenario

1013

$$Input'_{j \leftarrow i_{imp}, SSP}^{2050} = \text{Max}(Input_{j \leftarrow i_{imp}, SSP}^{2050} + NP_{i,SSP}^{2050} * \frac{Input_{j \leftarrow i_{dom}, SSP}^{2050}}{X_{i,SSP}^{2050}}; 0)$$

1014 Where:

1015  $Input'_{j \leftarrow i_{imp}, SSP}^{2050}$ : Adjusted imports by sector  $j$  from sector  $i$  in 2050 under the SSP scenario.

1016  $Input_{j \leftarrow i_{imp}, SSP}^{2050}$ : Original projected imports by sector  $j$  from sector  $i$  in 2050 under the SSP scenario.

1017  $NP_{i,SSP}^{2050}$ : net production sector  $i$  in 2050 for an SSP scenario

1018  $Input_{j \leftarrow i_{dom}, SSP}^{2050}$ : Total inputs required by sector  $j$  from domestic sector  $i$  in 2050 under the SSP scenario

1019

$$Input'_{j \leftarrow i_{dom}, SSP}^{2050} = Input_{j \leftarrow i_{dom}, SSP}^{2050} + Input_{j \leftarrow i_{imp}, SSP}^{2050} - Input'_{j \leftarrow i_{imp}, SSP}^{2050}$$

1020

1021 Where:

1022  $Input'_{j \leftarrow i_{dom}, SSP}^{2050}$ : Adjusted domestic inputs from sector  $i$  to sector  $j$  in 2050 under the SSP scenario

1023  $Input_{j \leftarrow i_{dom}, SSP}^{2050}$ : Original projected domestic inputs from domestic sector  $i$  to sector  $j$  in 2050 under the  
 1024 SSP scenario

1025  $Input_{j \leftarrow i_{imp}, SSP}^{2050}$ : Original projected imports by sector  $j$  from sector  $i$  in 2050 under the SSP scenario.

1026  $Input'_{j \leftarrow i_{imp}, SSP}^{2050}$ : Adjusted imports by sector  $j$  from sector  $i$  in 2050 under the SSP scenario.

1027

1028

$$D'_{i,SSP}^{2050} = FD_{i,SSP}^{2050} + \sum_j Input'_{j \leftarrow i, SSP}^{2050}$$

1029 Where:

1030  $D'_{i,SSP}^{2050}$ : Adjusted total demand of sector  $i$

1031  $FD_{i,SSP}^{2050}$ : final demand for sector  $i$  in 2050 for an SSP scenario

1032  $Input'_{j \leftarrow i, SSP}^{2050}$ : Adjusted input required by sector  $j$  from sector  $i$  in 2050 for an SSP scenario

1033

1034

$$X_i^{2050} = VA_{i,SSP}^{2050} + \sum_j Input_{i \leftarrow j,SSP}^{2050}$$

1035 Where:

1036  $X_i^{2050}$ : Adjusted total output of sector  $i$

1037  $Input_{i \leftarrow j,SSP}^{2050}$ : Adjusted input required by sector  $j$  from sector  $i$  in 2050 for an SSP scenario

1038  $VA_{i,SSP}^{2050}$ : projected value added of sector  $i$  in 2050 for an SSP scenario

1039

$$NP'_{i,SSP}^{2050} = X_{i,SSP}^{2050} - D_{i,SSP}^{2050}$$

1040 Where:

1041  $NP'_{i,SSP}^{2050}$ : adjusted net production sector  $i$  in 2050 for an SSP scenario

1042  $X_i^{2050}$ : adjusted total output of sector  $i$  in 2050 for an SSP scenario

1043  $D_i^{2050}$ : adjusted total demand of sector  $i$  in 2050 for an SSP scenario

1044

$$Input''_{i \leftarrow i_{imp},SSP}^{2050} = Input'_{i \leftarrow i_{imp},SSP}^{2050} - NP'_{i,SSP}^{2050}$$

1045 Where:

1046  $Input''_{i \leftarrow i_{imp},SSP}^{2050}$ : Further adjusted imports by sector  $j$  from sector  $i$  in 2050 under the SSP scenario

1047  $Input'_{i \leftarrow i_{imp},SSP}^{2050}$ : Adjusted imports by sector  $j$  from sector  $i$  in 2050 under the SSP scenario.

1048  $NP'_{i,SSP}^{2050}$ : adjusted net production sector  $i$  in 2050 for an SSP scenario

1049

1050

1051

1052 *if*  $Input''_{i \leftarrow i_{imp},SSP}^{2050} < 0$ :

$$FD'_{i,SSP}^{2050} = FD_{i,SSP}^{2050} + (-Input''_{i \leftarrow i_{imp},SSP}^{2050})$$

$$Input''_{i \leftarrow i_{imp},SSP}^{2050} = 0$$

1053 Where:

1054  $Input''_{i \leftarrow i_{imp},SSP}^{2050}$ : Further adjusted imports by sector  $j$  from sector  $i$  in 2050 under the SSP scenario

1055  $FD'_{i,SSP}^{2050}$ : Adjusted final demand for sector  $i$  in 2050 for an SSP scenario

1056  $FD_{i,SSP}^{2050}$ : Original final demand for sector  $i$  in 2050 for an SSP scenario

1057

1058 **Appendix C: Building Classification**1059 **Table C.1:** *Aggregation of land use classes*

Sector	LUISA Land Use Class
Forestry	Agro-forestry areas
	Broad-leaved forest
	Coniferous forest
	Mixed forest
Agriculture	Non irrigated arable land
	Permanently irrigated land
	Rice fields
	Vineyards
	Fruit trees and berry plantations
	Olive groves
	Pastures
	Annual crops associated with permanent crops
	Complex cultivation patterns
	Land principally occupied by agriculture

1060

1061 **Table C.2:** *classification of building footprints based on OSM and LUISA data*

Assigned footprint class	LUISA	OSM Landuse	OSM Amenities
Industrial	Industrial or commercial units	industrial	industrial
	Road and rail networks and associated land	construction	construction
	Major stations	military	military
	Port areas	quarry	quarry
	Airport areas	railway	railway

	Airport terminals	barn	barn
	Mineral extraction sites	greenhouse	greenhouse
	Dump sites	hangar	hangar
	Construction sites	garages	garages
Commercial		church	church
		commercial	commercial
		hospital	hospital
		hotel	hotel
		retail	retail
		school	school
		service	service
		synagogue	synagogue
		university	university
		supermarket	supermarket
		office	office
		mosque	mosque
		kindergarten	kindergarten
		social_facility	social_facility

---

**1063 Appendix D: Demand Change Through The Leontief Inverse**

1064 Additional demand pressures on the national construction sector and its supply chain are  
1065 derived from the direct structural losses. Cascading demand changes are found by multiplying  
1066 the demand increase in the construction sector equal to the reconstruction costs with the  
1067 Leontief inverse. The Leontief inverse, represented by  $(I-A)^{-1}$ , is created using the national  
1068 input-output tables. The input-output table is the basis for developing the technical coefficient  
1069 matrix  $A$ . This matrix formulates the direct input requirements for producing one output unit in  
1070 each sector. Each element  $a_{ij}$  in matrix  $A$  represents the input of sector  $i$  to sector  $j$ , divided by  
1071 the total output of  $j$ . Using this matrix, we can use the following equation to find the demand  
1072 changes across the economy.

$$\Delta x = (I - A)^{-1} \Delta f$$

1073 Where:

1074  $\Delta x$ : vector of total output change for each sector.

1075  $I$ : identity matrix

1076  $A$ : technical coefficient matrix

1077  $\Delta f$ : vector with demand change of each sector

1078

1079